A self-consistent quasilinear theory for collisionless relaxation to universal quasi-steady state attractors in cold dark matter halos

Uddipan Banik*
Department of Astrophysical Sciences, Princeton University, 112 Nassau Street, Princeton, NJ 08540, USA
Institute for Advanced Study, Einstein Drive, Princeton, NJ 08540, USA
Perimeter Institute for Theoretical Physics, 31 Caroline Street N., Waterloo, Ontario, N2L 2Y5, Canada

Amitava Bhattacharjee†
Department of Astrophysical Sciences, Princeton University, 112 Nassau Street, Princeton, NJ 08540, USA
(Dated: December 2, 2024)

Collisionless self-gravitating systems such as cold dark matter halos are known to harbor universal density profiles despite the intricate non-linear physics of hierarchical structure formation. The origin of these attractor states has been a persistent mystery, particularly because the physics of collective collisionless relaxation is not well understood. To solve this problem, we develop a self-consistent quasilinear theory in action-angle space for the collisionless relaxation of driven, inhomogeneous, self-gravitating systems by perturbing the governing Vlasov-Poisson equations. We obtain a quasilinear diffusion equation that describes the secular evolution of the mean coarse-grained distribution function f_0 of a halo due to the linear fluctuations induced by random perturbations in the force field. The density fluctuations are collectively dressed by self-gravity, a phenomenon that is described by the response matrix. Unlike previous studies, we treat collective dressing up to all orders. We show that well-known halo profiles commonly observed in N-body simulations, including the r^{-1} Navarro-Frenk-White (NFW) cusp, an Einasto central core, and the $r^{-1.5}$ prompt cusp (where r is the halocentric radius), all emerge as quasi-steady state attractor solutions of the quasilinear diffusion equation. The r^{-1} cusp, with $f_0 \sim (E-\Phi_c)^{-5/2}$ (E is the energy and Φ_c is the central potential), is a constant flux steady-state solution for small-scale white noise fluctuations. In other words it is a quasi-steady state profile for a constantly accreting massive halo perturbed by nearly uncorrelated fluctuations induced by substructure. It is an outcome of the universal nature of collective relaxation: lower energy and angular momentum particles attract more particles, gain higher effective mass and get less accelerated by the fluctuating force field. The zero-flux steady state solution that describes an isolated halo is an f_0 that is flat in energy, and the corresponding density profile can either be a central core or an $r^{-1.5}$ cusp depending on the inner boundary condition. The $r^{-1.5}$ cusp forms around a central dense object, e.g., a compact sub-halo or a black hole. In short, we demonstrate for the first time that these halo profiles emerge as quasi-steady state attractors of collisionless relaxation described by a self-consistent quasilinear theory.

I. INTRODUCTION

Collisionless systems governed by long-range interactions are known to harbor non-thermal, non-Maxwellian distribution functions. The two-body relaxation timescale can be extremely long in collisionless self-gravitating systems such as galaxies and cold dark matter (CDM) halos. Therefore, such systems do not attain the maximum entropy state of a Maxwellian distribution function (DF), mandated by Boltzmann's H-theorem, in any reasonable dynamical timescale. Yet it is known that collisionless systems relax to universal attractor states that are often characterized by power-law DFs. This process usually takes several dynamical timescales, but is often the outcome of a violent collisionless relaxation [1] that occurs rapidly over a dynamical time. Despite several attempts over the last few decades, the origin of these universal attractor states has remained a persistent mystery.

Collisionless self-gravitating systems are described by the coupled, non-linear Vlasov-Poisson equations in a manner analogous to collisionless electrostatic plasmas. The Vlasov equation describes the evolution of the fine-grained DF f under the action of the gravitational force, which is itself sourced by the density (zeroth velocity moment of the DF) through the Poisson equation. It is well known that the Vlasov equation admits a denumerably infinite set of Casimir invariants, of which the Boltzmann H-function (negative of the Boltzmann-Shannon entropy) is but one, and any positive definite function of the conserved quantities of the system is a valid steady state solution to the Vlasov equation (strong Jeans theorem). Why then do collisionless systems relax towards universal steady states? The answer lies in coarse-graining. The Vlasov equation evolves the fine-grained DF f. In reality, however, we can only measure the coarse-grained DF $f_0 = \langle f \rangle$, obtained by some kind of averaging of the fine-grained DF, be it from actual observations, which are limited by instrumental resolution, or in numerical experiments, which are limited by grid resolution. The Vlasov equation predicts extreme filamentation of the fine-grained DF with small-scale structures going all the way down to the free-streaming scale. The coarse-grained DF does not follow the Vlasov equation but a modified kinetic equation with a collision operator that encompasses the physics of Vlasov turbulence and kinetic instabilities. It is this effective collision operator that captures the small-scale (also known as sub-grid) physics of collective, collisionless relaxation and picks out a particular functional

* uddipan.banik@princeton.edu, uddipanbanik@ias.edu
† amitava@princeton.edu

form for the coarse-grained DF f_0 in the quasi-steady state. This effective description of collisionless relaxation is very much in the same spirit as the effective field theories of particle physics and large-scale structure/cosmology. The collision operator in the modified kinetic equation can be very different from the Boltzmann operator (for example, it can be the Balescu-Lenard operator [2])

The kinetic equation for the relaxation of the coarse-grained DF can be obtained using quasilinear theory (QLT), which involves perturbing the Vlasov-Poisson equations up to second order followed by coarse-graining (spatial averaging for homogeneous systems and orbit/phase averaging for inhomogeneous ones) of the DF. This yields a diffusion equation for the evolution of the coarse-grained DF due to the underlying force fluctuations. Such a quasilinear diffusion equation has been derived in the context of collisionless electrostatic plasmas by Banik *et al.* [3], and for collisionless systems governed by long range interactions in general by Chavanis [4, 5, 6], who refers to it as the secular dressed diffusion equation. In standard QLT, while the equation governing the time-evolution of the slowly evolving mean DF is exact, the fluctuations are assumed to obey linearized equations (when in reality, the fluctuations, too, obey nonlinear equations). The long time evolution of the coarse-grained DF, averaged over these fluctuations, is well-described by QLT if the quasilinear diffusion timescale is longer than the dynamical time of the system. In this paper we use QLT in the canonical action-angle variables [c.f. 7] to study the evolution of the coarse-grained DF f_0 of an inhomogeneous galaxy/halo. We perturb the Vlasov-Poisson equations to obtain the quasilinear diffusion equation that describes the relaxation of the *angle-averaged* or *phase-averaged DF* f_0. The key ingredient of this diffusion equation is the diffusion tensor, which depends on the fluctuation power-spectrum and the response matrix that encompasses the physics of collective effects.

What does f_0 look like in the fully non-linear setup? We get an idea from the cosmological N-body simulations of a CDM universe. It is difficult to measure f_0 precisely from these simulations due to the noise introduced by a finite number of simulation particles, but it is possible to measure its velocity moments, e.g., the density profile of a halo, which is the zeroth velocity moment of f_0 and is a smoother function. Early cosmological N-body simulations show a remarkable universality in the density profiles of CDM halos. Navarro *et al.* [8] find that the Navarro-Frenk-White (NFW) profile, $\rho(r) \sim r^{-1}\,(r + r_{\rm s})^{-2}$ ($r_{\rm s}$ is the scale radius), is an excellent fit to the halo density, irrespective of the halo mass and concentration, power-law index of the initial power spectrum and cosmology. Later simulations, however, predict more diversity in the halo profiles. Moore *et al.* [9] find that the inner halo harbors an $\sim r^{-1.4}$ cusp, much steeper than the NFW r^{-1} cusp. Navarro *et al.* [10], on the other hand, find that most halos show an inner r^{-1} cusp. Contrary to these results, high-resolution Aquarius [11] and Via Lactea II [12] simulations find that the inner log-slope of the density profile becomes progressively shallower than 1 towards the center, akin to the Einasto [13] profile. More recently, very high-resolution (zoom-in) cosmological simulations [14] have found the first halos to harbor steep $r^{-1.5}$ cusps akin to the Moore *et al.* [9] profile, which Delos and White [14] refer to as prompt cusps. They point out that many of these prompt cusps eventually assume Einasto or NFW-like profiles at intermediate radii when they grow in mass. All in all, whether there exist attractors in the landscape of halo profiles in N-body simulations is still subject to debate.

We address the question of universality of halo profiles by answering the following key question: how does a galaxy or halo respond to stochastic perturbations in the gravitational force field (e.g., sourced by other galaxies/halos or by substructure) and relax, and what are the accessible relaxed states? We model the collisionless relaxation of inhomogeneous self-gravitating systems using a quasilinear diffusion equation and find that the NFW, Einasto and prompt cusp-like profiles naturally emerge as its attractor steady-state solutions. Weinberg [15, 16] also solves the quasilinear diffusion equation, albeit for a limited range of initial galaxy profiles without a central cusp. He infers that weakly damped dipole modes excited by stochastic perturbations from orbiting satellites drive the secular relaxation of the halo towards a universal Einasto-like profile. Contrary to our prediction, he does not obtain the NFW r^{-1} cusp as an attractor state. We believe that the main reason for this discrepancy is that Weinberg [15, 16] assumes the collective dressing to be weak, i.e., dielectric tensor to be close to identity (see section [V] for details). However, to obtain the NFW cusp as a steady-state attractor of collisionless relaxation, one must properly realize the collective effects by incorporating the full linear response equation (up to all orders in the response matrix $\mathbb{M}$) in the QLT.

Our approach towards explaining the origin of halo profiles, while being similar to that of Weinberg [15] and [16], is fundamentally different from most other previous work. We develop an Eulerian framework for the self-consistent evolution of the coarse-grained DF (under the quasilinear assumption), while previous literature has mainly focused on a Lagrangian framework for the orbital evolution of individual particles in a time-varying potential with the assumption of self-similarity and approximations for the orbital configuration. The secondary infall model of [17] and [18] consists of a spherically symmetric self-similar solution for purely radial orbits that predicts an initial halo profile $\rho_i(r) \sim r^{-\gamma_{\rm i}}$ relaxing to a final halo profile $\rho(r) \sim r^{-\gamma_{\rm f}}$ with $\gamma_{\rm f} = 2$ for $\gamma_i \leq 2$ and $\gamma_{\rm f} = 3\gamma_{\rm i}/(1+\gamma_{\rm i})$ for $\gamma_{\rm i} > 2$. It is, however, well known that a collisionless system with purely radial orbits is unstable to the formation of non-axisymmetric dipole and quadrupole (bar) modes [19]. [20] found that for non-zero but constant specific angular momentum per particle, one can obtain the [17] and [18] slope of $\gamma_{\rm f} = 3\gamma_{\rm i}/(1+\gamma_{\rm i})$ for all γ_i. The steep slope of $\gamma_{\rm f} = 2$ for $\gamma_{\rm i} < 2$ is eliminated due to the centrifugal barrier and non-zero periapse of particles moving along non-radial orbits. Interestingly, [21] found using 1D simulations that imposing isotropization of the particle velocities during collapse results in $\gamma_{\rm f} = 1$ for $\gamma_{\rm i} \leq 0.5$, which they interpreted as a hint that the r^{-1} NFW cusp may originate from orbit isotropization through violent relaxation. [22] and [23] find that halos tend to relax towards a central cusp with $\gamma_{\rm f}$ slightly larger than 1. They argue that cored halos with $\gamma_{\rm f} < 1$ exert compressive tidal forces on the

infalling subhalos which therefore survive disruption and inspiral all the way to the center under dynamical friction, which results in $\gamma_{\rm f} \gtrsim 1$. This, however, does not take into account core-stalling [24, 25], the stalling of subhalo inspiral due to vanishing dynamical friction in cored galaxies, found in later high resolution idealized simulations [26–29]. [30] find that a self-similar solution with adiabatic invariance of the radial action yields a halo profile with a central core and a gradual Einasto-like roll-over of the log-slope akin to the halo profiles obtained from the high resolution Via Lactea II and Aquarius simulations.

Whether CDM halos possess a universal profile at all, and whether it is NFW-like, Einasto-like or prompt cusp-like or something else altogether, has been a matter of long-drawn controversy. This is mainly because the physics of collective, collisionless relaxation has remained poorly understood. We adopt an alternate route, fundamentally different from the above approaches but in the same spirit as [15] and [16]. Instead of looking at the evolution of the halo density profile directly, we build a QLT for the collisionless relaxation of the DF from first principles (Vlasov-Poisson equations), look for attractor steady-state solutions of the DF, and identify the halo density profiles corresponding to these attractor states from a unified perspective. The focus of our paper is not on the formation of the halo or the temporal evolution towards the attractor states (although QLT enables a description of the slow temporal evolution of the mean DF) but rather on the existence of such states. As alluded to earlier, we find that NFW, Einasto and prompt cusp-like profiles all emerge as quasi-steady state attractors of collisionless relaxation.

This paper is organized as follows. Section II introduces the perturbative (linear and quasilinear) response theory for the relaxation of driven collisionless self-gravitating systems governed by the Vlasov-Poisson equations. In Section III, we derive the quasilinear diffusion equation for the evolution of the mean coarse-grained DF of the halo. In section IV we obtain the steady state solution to this equation, showing that the NFW r^{-1} cusp is a constant flux solution while the Einasto-like central core and the $r^{-1.5}$ prompt cusp are zero flux solutions. We summarize our findings in section V.

II. RESPONSE THEORY FOR COLLISIONLESS SELF-GRAVITATING SYSTEMS

A self-gravitating system is characterized by the DF or phase space $(\mathbf{x}, \mathbf{v})$ density of its constituent particles, $f(\mathbf{x}, \mathbf{v}, t)$. The general equations governing the relaxation of a collisionless self-gravitating fluid such as a cold dark matter (CDM) halo or a galaxy are the collisionless Boltzmann or Vlasov and Poisson equations,

$$\begin{aligned} &\frac{\partial f}{\partial t} + [f, H] = 0, \\ &\nabla^2 \Phi = 4\pi G \int d^3v\, f. \end{aligned} \tag{1}$$

where $H = v^2/2 + \Phi$ denotes the Hamiltonian with Φ the gravitational potential and $[f, H]$ denotes the Poisson bracket. We describe the inhomogeneous galaxy or halo in terms of the canonical angle-action variables, $(\mathbf{w}, \mathbf{I})$, with $\mathbf{I} = (I_r, L, L_z)$, where I_r is the radial action, L the angular momentum and L_z the z component of the angular momentum. The Poisson bracket is given by $[f, H] = \nabla_{\mathbf{w}} f \cdot \nabla_{\mathbf{I}} H - \nabla_{\mathbf{I}} f \cdot \nabla_{\mathbf{w}} H$.

We study the response of the system to an external perturber potential $\Phi_{\rm P}$ sourced by other galaxies or halos or by substructure within the system. The Hamiltonian can then be written as $H = H_0 + \Phi_{\rm P} + \Phi'$ with $H_0 = v^2/2 + \Phi_0$, Φ_0 the quasi-equilibrium galaxy/halo potential and Φ' the self-consistent potential sourced by the response itself through the Poisson equation. The Vlasov equation is difficult to solve in its full generality due to the non-linearity in both $\mathbf{w}$ and $\mathbf{I}$, and hence, one must resort to perturbation theory to obtain analytical solutions. If the strength of the perturber potential, $\Phi_{\rm P}$, is smaller than σ_0^2, where σ_0 is the velocity dispersion of the unperturbed quasi-equilibrium system, then the perturbation in f can be expanded as a power series in the perturbation parameter, $\epsilon \sim |\Phi_{\rm P}|/\sigma_0^2$, i.e., $f = f_0 + \epsilon f_1 + \epsilon^2 f_2 + \ldots$; the self-consistent potential Φ' can also be expanded accordingly as $\Phi' = \epsilon\Phi_1 + \epsilon^2\Phi_2 + \ldots$.

A. Linear response theory

The first-order response of the system to the perturber is described by the linearized Vlasov-Poisson equations,

$$\begin{aligned} &\frac{\partial f_1}{\partial t} + [f_1, H_0] + [f_0, \Phi_{\rm P}] + [f_0, \Phi_1] = 0, \\ &\nabla^2 \Phi_1 = 4\pi G \int d^3v\, f_1. \end{aligned} \tag{2}$$

Assuming that the unperturbed, quasi-equilibrium f_0 is phase/angle-averaged, i.e., only a function of the actions (strong Jeans theorem), expanding the linear quantities as Fourier series in angles, performing the Laplace transform in time, and expanding the Fourier-Laplace coefficients in terms of bi-orthogonal basis functions as outlined in Appendix A, we obtain the following response equation:

$$\tilde{\mathbf{a}}(\omega) = (\mathbb{I} - \mathbb{M}(\omega))^{-1} \mathbb{M}(\omega)\, \tilde{\mathbf{b}}(\omega), \tag{3}$$

where tilde indicates the Laplace transform, $\mathbb{I}$ denotes the identity matrix, and $\mathbb{M}$ indicates the response matrix given by

$$\mathbb{M}_{pq}(\omega) = \frac{(2\pi)^3}{4\pi G} \sum_{\boldsymbol{\ell}} \int \mathrm{d}\mathbf{I}\, \boldsymbol{\ell} \cdot \frac{\partial f_0}{\partial \mathbf{I}} \frac{\psi^{(p)*}_{\boldsymbol{\ell}}(\mathbf{I}) \psi^{(q)}_{\boldsymbol{\ell}}(\mathbf{I})}{\omega - \boldsymbol{\ell} \cdot \Omega}. \tag{4}$$

The matrix, $(\mathbb{I} - \mathbb{M})$, denotes the dielectric tensor. $\psi^{(p)}_{\boldsymbol{\ell}}(\mathbf{I})$ denotes the Fourier coefficient (of the $\boldsymbol{\ell}$ mode) with respect to the angles of the basis function $\psi^{(p)}(\mathbf{x})$, in which the potentials are expanded as $\Phi_1(\mathbf{x}, t) = \sum_p a_p(t)\psi^{(p)}(\mathbf{x})$ and $\Phi_{\rm P}(\mathbf{x}, t) =$

$\sum_p b_p(t)\psi^{(p)}(\mathbf{x})$. $\tilde{\mathbf{a}}$ ($\tilde{\mathbf{b}}$) denotes the Laplace transform of $\mathbf{a}$ ($\mathbf{b}$). Equation (3) manifests the dressing of the response to the perturber by the polarization of the medium due to self-gravity. The response matrix, which would be zero in the absence of self-gravity, encodes the information about this dressing. Particles gravitationally interact with each other, which increases their inertia and causes them to experience the dressed and not the bare potential. Performing the inverse Laplace transform of the response equation (3) shows that the temporal response of the $\boldsymbol{\ell}$ mode consists of three terms: a continuum response that oscillates as $\exp[-i\boldsymbol{\ell}\cdot\boldsymbol{\Omega}t]$, a forced response or wake that follows the temporal dependence of the perturber (responsible for dynamical friction [24, 31–34]) and a set of coherent oscillations or Landau modes oscillating at frequencies ω_n that follow the dispersion relation $\det(\mathbb{I}-\mathbb{M}(\omega_n))=0$ (see Appendix A for a detailed derivation).

B. Second-order response theory

The second-order response of the system is described by the following evolution equations for f_2 and Φ_2:

$$\frac{\partial f_2}{\partial t}+[f_2,H_0]+[f_1,\Phi_{\rm P}]+[f_1,\Phi_1]+[f_0,\Phi_2]=0,$$
$$\nabla^2\Phi_2=4\pi G\int d^3v\, f_2. \tag{5}$$

The evolution of f_2 is guided by that of the linear fluctuations, f_1 and Φ_1, which we have already computed using linear response theory. As before, we can evolve the above equations in the Fourier space of angles. The evolution of the mean background DF, averaged over the angles and the random phases of the linear fluctuations, $f_{2\boldsymbol{\ell}=0}=f_0$, can be studied by taking the $\boldsymbol{\ell}\to 0$ limit of the second order response, $f_{2\boldsymbol{\ell}}$, which yields (see Appendix B for details)

$$\frac{\partial f_0}{\partial t}=i\sum_{\boldsymbol{\ell}}\boldsymbol{\ell}\cdot\frac{\partial}{\partial\mathbf{I}}\left\langle f^*_{1\boldsymbol{\ell}}(\mathbf{I},t)\,\Phi_{\boldsymbol{\ell}}(\mathbf{I},t)\right\rangle. \tag{6}$$

Here, $f_{1\boldsymbol{\ell}}$ is the Fourier coefficient of f_1, while $\Phi_{\boldsymbol{\ell}}$ is equal to $\Phi_{\rm P\boldsymbol{\ell}}+\Phi_{1\boldsymbol{\ell}}$, $\Phi_{\rm P\boldsymbol{\ell}}$ and $\Phi_{1\boldsymbol{\ell}}$ being the Fourier coefficients of $\Phi_{\rm P}$ and Φ_1 respectively. The brackets denote an ensemble average over the random phases of the fluctuations. The unperturbed mean DF f_0 is not a stationary quantity, rather it evolves secularly on a timescale longer than the mean dynamical time via the above quasilinear equation [see 35, for a comprehensive review of QLT]. Upon substituting the expressions for $f_{1\boldsymbol{\ell}}$ and $\Phi_{\boldsymbol{\ell}}$ obtained using linear response theory in the above equation, and taking the long time limit such that the Landau modes have damped away (assuming there are no instabilities), we obtain the following form for the quasilinear equation (see Appendix B for a detailed derivation):

$$\frac{\partial f_0}{\partial t}=\sum_{\boldsymbol{\ell}}\boldsymbol{\ell}\cdot\frac{\partial}{\partial\mathbf{I}}\left(D_{\boldsymbol{\ell}}(\mathbf{I})\,\boldsymbol{\ell}\cdot\frac{\partial f_0}{\partial\mathbf{I}}\right), \tag{7}$$

with $D_{\boldsymbol{\ell}}(\mathbf{I})$ given by

$$D_{\boldsymbol{\ell}}(\mathbf{I})=\left|(\mathbb{I}-\mathbb{M}(\boldsymbol{\ell}\cdot\boldsymbol{\Omega}))^{-1}_{pq}B_q\psi^{(p)}_{\boldsymbol{\ell}}(\mathbf{I})\right|^2 C_\omega(\boldsymbol{\ell}\cdot\boldsymbol{\Omega}), \tag{8}$$

and the Einstein summation convention implied. Here we take the perturber potential to be a generic red noise:

$$\left\langle b^*_q(t)\,b_{q'}(t')\right\rangle=B^*_qB_{q'}C_t(t-t'), \tag{9}$$

with C_t the temporal correlation function that is equal to $\delta(t-t')$ for white/uncorrelated noise. The Fourier transform of the correlation function is given by C_ω, which, for white noise, is simply equal to 1.

III. QUASILINEAR THEORY FOR COLLISIONLESS RELAXATION

Now we study the collisionless relaxation of the galaxy/halo by evolving the phase-averaged DF f_0 via the quasilinear equation (7), which can be recast into the following form of a *diffusion equation*:

$$\frac{\partial f_0}{\partial t}=\frac{\partial}{\partial I_i}\left(D_{ij}(\mathbf{I})\,\frac{\partial f_0}{\partial I_j}\right), \tag{10}$$

with the diffusion tensor D_{ij} given by

$$D_{ij}(\mathbf{I})=\sum_{\boldsymbol{\ell}}\ell_i\ell_j\left|(\mathbb{I}-\mathbb{M}(\boldsymbol{\ell}\cdot\boldsymbol{\Omega}))^{-1}_{pq}B_q\psi^{(p)}_{\boldsymbol{\ell}}(\mathbf{I})\right|^2, \tag{11}$$

and the response matrix $\mathbb{M}_{pq}$ given by

$$\mathbb{M}_{pq}(\boldsymbol{\ell}\cdot\boldsymbol{\Omega})=\frac{(2\pi)^3}{4\pi G}\sum_{\boldsymbol{\ell}'}\int d\mathbf{I}'\,\boldsymbol{\ell}'\cdot\frac{\partial f_0}{\partial\mathbf{I}'}\,\frac{\psi^{(p)*}_{\boldsymbol{\ell}'}(\mathbf{I}')\psi^{(q)}_{\boldsymbol{\ell}'}(\mathbf{I}')}{\boldsymbol{\ell}\cdot\boldsymbol{\Omega}-\boldsymbol{\ell}'\cdot\boldsymbol{\Omega}'}. \tag{12}$$

Here we have assumed that the external perturbation acts as a white noise, for which $C_\omega=1$. In other words, any two subsequent perturbations are uncorrelated, or even if they are correlated, the correlation time is smaller than the orbital time $\sim 2\pi/\boldsymbol{\ell}\cdot\boldsymbol{\Omega}$ at $\mathbf{I}$. We also assume that all Landau modes have damped away. This implicitly assumes that we are looking at the long time relaxation of the system at $t\gtrsim 1/\gamma_0$, where γ_0 is the damping rate of the least damped Landau mode. Under these assumptions, we find that f_0 evolves under the above quasilinear diffusion equation, also known as the secular dressed diffusion equation [4–6]. In fusion plasma physics, a similar formulation of QLT using action-angle variables was pioneered by Kaufman [36].

Let us now make the simplifying assumption that f_0 is spherically symmetric and isotropic in the velocity space, in which case f_0 can be described as a function of the energy E, i.e., f_0 is an ergodic distribution $f_0(E)$ [37]. This enables us

to rewrite $\boldsymbol{\ell}\cdot\partial f_0/\partial\mathbf{I}$ as $\boldsymbol{\ell}\cdot\boldsymbol{\Omega}\,\partial f_0/\partial E$, which reduces the above quasilinear diffusion equation into the following one dimensional diffusion equation in energy:

$$\frac{\partial f_0}{\partial t} = \sum_{\boldsymbol{\ell}} \boldsymbol{\ell}\cdot\boldsymbol{\Omega}\frac{\partial}{\partial E}\left(\boldsymbol{\ell}\cdot\boldsymbol{\Omega}\, D_{\boldsymbol{\ell}}\left(\mathbf{I}\right)\frac{\partial f_0}{\partial E}\right), \tag{13}$$

with $D_{\boldsymbol{\ell}}$ given by

$$D_{\boldsymbol{\ell}}\left(\mathbf{I}\right) = \left|\left(\mathbb{I}-\mathbb{M}\left(\boldsymbol{\ell}\cdot\boldsymbol{\Omega}\right)\right)^{-1}_{pq} B_q \psi^{(p)}_{\boldsymbol{\ell}}\left(\mathbf{I}\right)\right|^2, \tag{14}$$

and $\mathbb{M}_{pq}$ given by

$$\mathbb{M}_{pq}\left(\boldsymbol{\ell}\cdot\boldsymbol{\Omega}\right) = \frac{(2\pi)^3}{4\pi G}\sum_{\boldsymbol{\ell}'}\int \mathrm{d}\mathbf{I}'\frac{\partial f_0}{\partial E'}\,\psi^{(p)*}_{\boldsymbol{\ell}'}(\mathbf{I}')\psi^{(q)}_{\boldsymbol{\ell}'}(\mathbf{I}')$$
$$\times\left[\left(\frac{\boldsymbol{\ell}\cdot\boldsymbol{\Omega}}{\boldsymbol{\ell}'\cdot\boldsymbol{\Omega}'}-1\right)^{-1} - i\pi\,\boldsymbol{\ell}'\cdot\boldsymbol{\Omega}'\delta\left(\boldsymbol{\ell}\cdot\boldsymbol{\Omega}-\boldsymbol{\ell}'\cdot\boldsymbol{\Omega}'\right)\right] \tag{15}$$

Here we have used the fact that $\boldsymbol{\Omega} = \partial H_0/\partial\mathbf{I} = \partial E/\partial\mathbf{I}$, and split up the integral in the expression for the response matrix given in equation (12) into the principal value and the residue at the pole.

We have successfully reduced the original diffusion equation (10) to a one-dimensional diffusion equation. But $D_{\boldsymbol{\ell}}\left(\mathbf{I}\right)$ and $\boldsymbol{\Omega}$ explicitly depend on all the action variables unlike f_0 that depends on $\mathbf{I}$ implicitly through E. Therefore, further simplification is due before we attempt a solution. We adopt $\psi^{(p)}(r) \sim \exp\left[ipk_r r\right]/r$ with a characteristic wavenumber k_r as a complete orthogonal basis for spherically symmetric perturbations to a spherical halo. If the size of the halo is equal to $R_{\rm h}$, then k_r is of order $1/R_{\rm h}$. If the minimum and maximum wavenumbers of the perturber are $k_{\rm min}$ and $k_{\rm max}$ respectively, then $k_{\rm min}/k_r \le p \le k_{\rm max}/k_r$. We compute $\psi^{(p)}_{\boldsymbol{\ell}}$ for this set of basis functions in Appendix C. We show that $\psi^{(p)}_{\boldsymbol{\ell}}(\mathbf{I}) \sim \exp\left[ipk_r R_{\rm c}\right]\zeta^{(p)}_{\boldsymbol{\ell}}\left(I_r, k_r, R_{\rm c}\right)/R_{\rm c}$ in this case, with $R_{\rm c}(L)$ the circular radius for angular momentum L and ζ a function involving Bessel functions of the first kind that is peaked around small I_r, especially for small-scale perturbations with $pk_rR_{\rm c} \gtrsim 1$. For a given L_z, and at small I_r, the diffusion equation (13) can be rewritten as the following *reduced diffusion equation*:

$$\frac{\partial f^{(\rm c)}_0}{\partial t} = \sum_{\boldsymbol{\ell}} \boldsymbol{\ell}\cdot\boldsymbol{\Omega}_{\rm c}\frac{\partial}{\partial E_{\rm c}}\left(\boldsymbol{\ell}\cdot\boldsymbol{\Omega}_{\rm c}\, D^{(\rm c)}_{\boldsymbol{\ell}}\left(E_{\rm c}\right)\frac{\partial f^{(\rm c)}_0}{\partial E_{\rm c}}\right), \tag{16}$$

with

$$\begin{aligned} E_{\rm c} &= E\left(L_{\rm c}, I_r\approx 0\right),\\ \boldsymbol{\Omega}_{\rm c} &= \boldsymbol{\Omega}\left(L_{\rm c}, I_r\approx 0\right) = \boldsymbol{\Omega}\left(E_{\rm c}, L_{\rm c}\right),\\ f^{(\rm c)}_0 &= f_0(L_{\rm c}, I_r\approx 0) = f_0(E_{\rm c}), \end{aligned} \tag{17}$$

and

$$D^{(\rm c)}_{\boldsymbol{\ell}} = \frac{1}{R^2_{\rm c}}\left|\left(\mathbb{I}-\mathbb{M}\left(\boldsymbol{\ell}\cdot\boldsymbol{\Omega}_{\rm c}\right)\right)^{-1}_{pq} B_q\,\zeta^{(p)}_{\boldsymbol{\ell}}\left(I_r, k_r, R_{\rm c}\right)\right|^2,$$
$$\mathbb{M}_{pq}\left(\boldsymbol{\ell}\cdot\boldsymbol{\Omega}_{\rm c}\right) \approx \frac{(2\pi)^3}{4\pi G}\sum_{\boldsymbol{\ell}'}\left(\mathbb{M}^{(1)}_{\boldsymbol{\ell}' pq} + \mathbb{M}^{(2)}_{\boldsymbol{\ell}' pq}\right),$$
$$\mathbb{M}^{(1)}_{\boldsymbol{\ell}' pq} = \frac{C_{\boldsymbol{\ell}' pq}}{k_r^2}$$
$$\times\int \mathrm{d}L'_{\rm c}\,\frac{\kappa' L'_{\rm c}}{R'^2_{\rm c}}\left(\frac{\boldsymbol{\ell}\cdot\boldsymbol{\Omega}_{\rm c}}{\boldsymbol{\ell}'\cdot\boldsymbol{\Omega}'_{\rm c}}-1\right)^{-1}\frac{\partial f^{(\rm c)}_0}{\partial E'_{\rm c}}\exp\left[-i\left(p-q\right)k_r R'_{\rm c}\right],$$
$$\mathbb{M}^{(2)}_{\boldsymbol{\ell}' pq} = -i\pi\frac{\kappa L_{\rm c} D_{\boldsymbol{\ell}\boldsymbol{\ell}' pq}}{k_r^2 R_{\rm c}^2}$$
$$\times\left(\frac{\partial\ln\boldsymbol{\ell}\cdot\boldsymbol{\Omega}_{\rm c}}{\partial L_{\rm c}}\right)^{-1}\frac{\partial f^{(\rm c)}_0}{\partial E_{\rm c}}\exp\left[-i\left(p-q\right)k_r R_{\rm c}\right]. \tag{18}$$

Here, $C_{\boldsymbol{\ell}' pq}$ and $D_{\boldsymbol{\ell}\boldsymbol{\ell}' pq}$ are constants that arise from integrating over I'_r and L'_z, and $\kappa = \Omega_r\left(L_{\rm c}, I_r\to 0\right)$ is the radial epicyclic frequency. The subscript c denotes that the quantities are evaluated on a nearly circular orbit with $I_r \approx 0$. The factor $\kappa' L'_{\rm c}/k_r^2 R'^2_{\rm c}$ arises from the integration over I'_r and L'_z. Note that the Einstein summation convention is not implied in $\mathbb{M}^{(1)}_{pq}$ and $\mathbb{M}^{(2)}_{pq}$. We have assumed that $\Psi^{(p)}_{\boldsymbol{\ell}}$ dominates at small I_r, since this is typically the case for small-scale perturbations, i.e., $pk_rR_{\rm c} \gtrsim 1$ (see Appendix C), which is the case of interest in this paper. We show in Appendix C that the diagonal terms of $\mathbb{M}_{pq}$ dominate over the off-diagonal terms for $pk_rR_{\rm c} \gtrsim 1$ and $qk_rR_{\rm c} \gtrsim 1$. This is an essential feature of small-scale fluctuations or the WKB limit.

IV. STEADY STATE SOLUTION

Our choice of a convenient form for the basis functions that applies to spherically symmetric perturbations, and the assumption of velocity isotropy, have simplified the complicated quasilinear diffusion equation (10) to the analytically tractable reduced diffusion equation (16). Now we look for its steady-state solutions. We only consider steady-state DFs that are linearly stable to perturbations, i.e., have $\partial f_0/\partial E \le 0$, according to the Antonov criterion [37], in which case they become steady state attractors.

Putting the RHS of equation (16) to zero, we obtain the following equation for the steady state $f^{(\rm c)}_0$:

$$\sum_{\boldsymbol{\ell}} \boldsymbol{\ell}\cdot\boldsymbol{\Omega}_{\rm c}\frac{\partial}{\partial E_{\rm c}}\left(\boldsymbol{\ell}\cdot\boldsymbol{\Omega}_{\rm c}\, D^{(\rm c)}_{\boldsymbol{\ell}}\left(E_{\rm c}\right)\frac{\partial f^{(\rm c)}_0}{\partial E_{\rm c}}\right) = 0, \tag{19}$$

with $D^{(\rm c)}_{\boldsymbol{\ell}}$ and $\mathbb{M}_{pq}\left(\boldsymbol{\ell}\cdot\boldsymbol{\Omega}\right)$ given by equations (18). The above set of equations admits an entire family of steady state solutions. These can be categorized into constant flux and zero flux solutions, which we examine separately as follows.

A. Constant flux solution

One possible way to fulfill the steady state condition given in equation (19) is the presence of a constant current or flux for each $\boldsymbol{\ell}$ mode, i.e.,

$$\boldsymbol{\ell}\cdot\boldsymbol{\Omega}_{\rm c}\, D^{(\rm c)}_{\boldsymbol{\ell}}\left(E_{\rm c}\right)\frac{\partial f^{(\rm c)}_0}{\partial E_{\rm c}} = \text{constant}, \tag{20}$$

independent of the circular energy $E_{\rm c}$ (or equivalently the circular angular momentum $L_{\rm c}$ or the circular radius $R_{\rm c}$). We look for solutions that allow for the equilibrium density profile of a spherically symmetric halo to scale as $\rho_0(r)\sim r^{-\gamma}$ in the inner region. Before attempting to obtain such a steady state solution, we require the following essential ingredients: the functional dependencies of $E_{\rm c}$, $\boldsymbol{\Omega}_{\rm c}$ and $f^{(\rm c)}_0$ on $L_{\rm c}$ or $R_{\rm c}$. This point is discussed below.

The equilibrium density $\rho_0(r)\sim r^{-\gamma}$ is related to the equilibrium galaxy potential $\Phi_0(r)$ through the spherically symmetric Poisson equation:

$$\frac{1}{r^2}\frac{\rm d}{{\rm d}r}\left(r^2\Phi_0(r)\right) = 4\pi G\rho_0(r). \tag{21}$$

It can be easily seen that the potential scales as $\Phi_0(r)\sim\Phi_{\rm c}\left(1-(r/r_{\rm s})^{2-\gamma}\right)$ for $r<r_{\rm s}$, with $r_{\rm s}$ the scale radius and $\Phi_{\rm c}$ the central potential, provided that $\gamma<2$ such that the enclosed mass $M_0(r)=4\pi\int_0^r {\rm d}r'\,r'^2\rho_0(r')$ is finite at $r\to 0$. As a function of the circular radius $R_{\rm c}$, the potential $\Phi_0(R_{\rm c})$ therefore scales as $\sim\Phi_{\rm c}\left(1-(R_{\rm c}/r_{\rm s})^{2-\gamma}\right)$. The energy $E_{\rm c}$ of a circular orbit scales in the same way. The azimuthal frequency Ω_ϕ is equal to $\sqrt{\Phi'\left(R_{\rm c}\right)/R_{\rm c}}$, and scales as $\Omega_0(R_{\rm c}/R_0)^{-\gamma/2}$ with Ω_0 and R_0 the characteristic frequency and radius of the halo. Similarly, the radial frequency Ω_R, equal to the epicyclic frequency $\kappa=\sqrt{R_{\rm c}\,{\rm d}\Omega^2_\phi/{\rm d}R_{\rm c}+4\Omega^2_\phi}=\sqrt{\Phi''\left(R_{\rm c}\right)+3\Phi'\left(R_{\rm c}\right)/R_{\rm c}}$, scales as $\kappa_0(R_{\rm c}/R_0)^{-\gamma/2}$ with $\kappa_0=c\,\Omega_0$ and c an $O(1)$ constant that varies between 1 and 2 [37]. The circular angular momentum, $L_{\rm c}=R^2_{\rm c}\Omega_\phi$, scales as $R^{2-\gamma/2}_{\rm c}$. The equilibrium DF can be obtained by Eddington inversion of the density profile [37], and can be shown to scale as [38]

$$f^{(\rm c)}_0\left(E_{\rm c}\right)\sim\left(E_{\rm c}-\Phi_{\rm c}\right)^{-\frac{6-\gamma}{2(2-\gamma)}}\sim R_{\rm c}^{\frac{\gamma}{2}-3}. \tag{22}$$

Plugging in the above scalings in the expression for the response matrix given in the second of equations (18), we find that for $pk_rR_{\rm c}\gtrsim 1$ and $qk_rR_{\rm c}\gtrsim 1$, $\mathbb{M}_{pq}$ scales as

$$\mathbb{M}_{pq}\left(\boldsymbol{\ell}\cdot\boldsymbol{\Omega}_{\rm c}\right)\sim\mathcal{A}_{\boldsymbol{\ell}pq}+\left(k_rR_{\rm c}\right)^{-3}\left(\mathcal{B}_{\boldsymbol{\ell}pq}+iC_{\boldsymbol{\ell}pq}\right), \tag{23}$$

with $\mathcal{A}_{\boldsymbol{\ell}pq}$, $\mathcal{B}_{\boldsymbol{\ell}pq}$ and $C_{\boldsymbol{\ell}pq}$ constants independent of $R_{\rm c}$. Only the diagonal terms of the dielectric tensor $(\mathbb{I}-\mathbb{M})_{pq}$ survive in this limit (see Appendix C 2). From the above expression it is evident that, for $k_rR_{\rm c}\lesssim 1$, i.e., within the halo, $\mathbb{M}_{pq}$ scales as $\sim\left(k_rR_{\rm c}\right)^{-3}$ as long as we consider perturbations acting on scales smaller than $R_{\rm c}$ with $pk_rR_{\rm c}\gtrsim 1$ and $qk_rR_{\rm c}\gtrsim 1$, i.e., $k_{\rm min}\gtrsim 1/R_{\rm c}$. In other words, this scaling shows up as long as B_p, the amplitude of the perturbation, dominates at $p\gtrsim 1/k_rR_{\rm c}$, i.e., on scales smaller than $R_{\rm c}$. For larger scale perturbations, i.e., for either $pk_rR_{\rm c}\lesssim 1$ or $qk_rR_{\rm c}\lesssim 1$, $\mathbb{M}_{pq}$ is of order unity. Therefore, only the small-scale perturbations are subject to significant collective dressing.

Since the dielectric tensor $(\mathbb{I}-\mathbb{M})_{pq}$ scales as $\sim R^{-3}_{\rm c}$ for small-scale perturbations, the reduced diffusion coefficient $D^{(\rm c)}_{\boldsymbol{\ell}}$ scales as $\sim R^{-2}_{\rm c}|\mathbb{I}-\mathbb{M}|^{-2}\sim R^4_{\rm c}$. And since $\boldsymbol{\Omega}_{\rm c}$ scales as $\sim R^{-\gamma/2}_{\rm c}$, $E_{\rm c}$ as $\sim R^{2-\gamma}_{\rm c}$, $f^{(\rm c)}_0$ as $\sim R^{\gamma/2-3}_{\rm c}$ and $\partial f^{(\rm c)}_0/\partial E_{\rm c}$ as $\sim R^{3\gamma/2-5}_{\rm c}$, we can substitute these scalings in the steady state condition given by equation (20), which yields

$$\begin{aligned} R_{\rm c}^{-\frac{\gamma}{2}+\left(\frac{3\gamma}{2}-5\right)+4} &= \text{constant}\\ \implies R_{\rm c}^{\gamma-1} &= \text{constant}. \end{aligned} \tag{24}$$

This implies that a constant flux steady state solution is a halo profile with

$$\gamma = 1. \tag{25}$$

Hence, we see that a halo that is forced by small-scale white noise-like fluctuations may tend towards an NFW-like $\gamma=1$ cusp in the quasi-steady state, as long as there is a constant flux of matter into the halo, or in other words the halo is accreting at a constant rate. The assumption of white noise is valid as long as the correlation time of the perturbations is shorter than $\sim 1/\boldsymbol{\ell}\cdot\boldsymbol{\Omega}$, i.e., the local orbital time. This is typically the case for small-scale fluctuations. The dominance of small-scale perturbations is crucial for the emergence of the NFW cusp, since it is this condition that results in the $\sim\left(k_rR_{\rm c}\right)^{-3}$ scaling of the response matrix, or strong collective dressing of the fluctuations, that ultimately gives rise to the r^{-1} density cusp. The key feature of collective dressing is the following. Lower angular momentum particles gather more neighbors and get more dressed, thereby acquiring higher effective mass and undergoing less acceleration due to the perturbing forces. The small-scale white noise-like fluctuations arise from the substructure within the halo itself. This, however, requires the halo to harbor a sufficiently large amount of substructure, which is only the case for more massive halos (e.g., a Milky Way sized halo). The above arguments suggest that the inner profile of massive halos that are accreting at a constant rate should evolve towards an NFW-like r^{-1} cusp due to collective collisionless relaxation under the action of substructure induced white noise perturbations.

B. Zero flux solution

The NFW cusp is not the only steady state of collisionless relaxation. What we have shown so far is that if the quasi-equilibrium density profile of a constantly accreting, spherically symmetric and isotropic halo scales as $\sim r^{-\gamma}$, then, under small-scale, white noise-like forcing, the only steady state

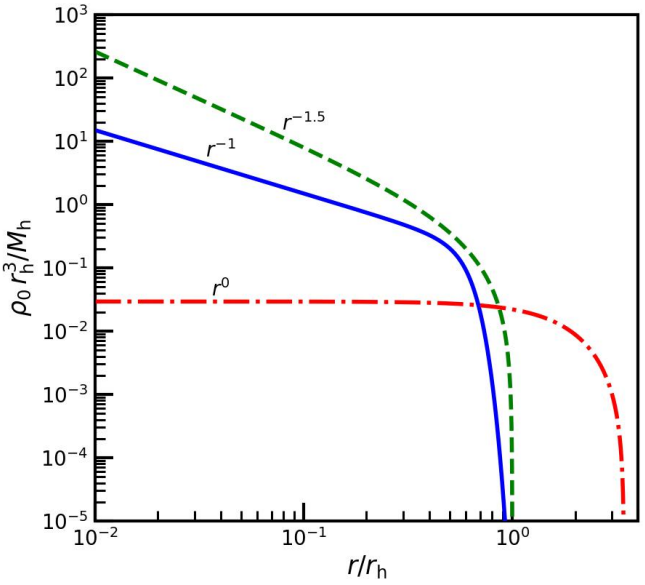

FIG. 1: Halo density ρ_0 (in units of M_h/r_h^3) as a function of radius r (in units of a characteristic radius r_h), normalized such that M_h is the total halo mass. The solid blue line indicates the constant flux steady state solution of the quasilinear diffusion equation (16): the r^{-1} NFW cusp (truncated by a Gaussian fall-off at $r \approx r_h$ so as to keep the halo mass finite). The dot-dashed red and dashed green lines indicate the central core and $r^{-1.5}$ profiles obtained by numerically integrating the Lane-Emden equation (28). These are the zero flux steady state solutions of equation (16).

solution is $\gamma = 1$. This does not preclude the possibility of other equilibrium halo profiles though. In fact, if the net flux of material is zero, i.e., the system is isolated, then a trivial way to satisfy the steady state condition is to require that

$$\boldsymbol{\ell} \cdot \boldsymbol{\Omega}_c \, D_\ell^{(c)}(E_c) \, \frac{\partial f_0^{(c)}}{\partial E_c} = 0 \implies \frac{\partial f_0^{(c)}}{\partial E_c} = 0, \qquad (26)$$

which is satisfied if $f_0(E)$ is a constant. The trivial solution is therefore that the DF is flat in energy space. In this case, the density ρ_0 can be simply obtained in terms of the galaxy potential as follows:

$$\rho_0 = 4\pi \int_0^{\sqrt{2\Psi_0}} \mathrm{d}\mathcal{E}\, \sqrt{2\,(\Psi_0 - \mathcal{E})}\, f_0 \sim \Psi_0^{3/2}, \qquad (27)$$

with $\mathcal{E} = -E$ and $\Psi_0 = -\Phi_0$, and $\sqrt{2\Psi_0}$ the escape velocity. This reduces the Poisson equation to the following Lane-Emden equation of order $n = 3/2$:

$$\frac{1}{s^2}\frac{\mathrm{d}}{\mathrm{d}s}\left(s^2 \frac{\mathrm{d}\psi}{\mathrm{d}s}\right) = -\psi^{3/2}, \qquad (28)$$

with $\psi = \Psi_0/\Psi_h$ and $s = r/r_h$, Ψ_h and r_h being characteristic (negative) potential and scale radius of the halo respectively. The above equation has two solutions for two sets of boundary conditions. If ψ tends to a constant and $\mathrm{d}\psi/\mathrm{d}s \to 0$ at $s \to 0$, then both ψ and ρ_0 follow a cored profile with a compact support that is truncated at some radius. The halo profile therefore harbors a central core akin to an Einasto profile but is truncated. On the other hand, if $\psi \sim s^{-1}$ at $s \to 0$, then ψ scales as s^{-1} for a large range in s before falling off to zero at some radius. The corresponding ρ_0 scales as $s^{-3/2}$, much like the prompt cusp, before truncation. This might happen if the halo centers around a massive compact subhalo with a density profile falling off more steeply than r^{-3}, or if the halo assembles around a black hole. In fact, this $r^{-3/2}$ profile emerges naturally as a self-similar solution of the infall of collisionless fluid onto a black hole in the secondary infall model of [18]. Fig. 1 plots the NFW-like r^{-1} profile as a solid blue line, and the Einasto-like cored and prompt cusp-like $r^{-3/2}$ profiles, obtained by numerically integrating equation (28), respectively as dot-dashed red and dashed green lines as a function of r. The profiles have been normalized by the halo mass M_h. The r^{-1} profile has been artificially truncated with a Gaussian fall-off around $r/r_h = 1$ so that the halo mass is finite.

V. DISCUSSION AND SUMMARY

We have developed a self-consistent quasilinear theory for the collisionless relaxation of CDM halos and galaxies. Using this theory, we have shown that while the evolution of the fine-grained DF is described by the Vlasov equation, that of the coarse-grained DF f_0 is governed by a Fokker-Planck type diffusion equation. It describes how the non-linear coupling of the dressed linear fluctuations sourced by stochastic perturbations in the gravitational potential drives the secular evolution of f_0 over timescales longer than the dynamical time. The steady state solution to this diffusion equation yields the quasi-equilibrium f_0 towards which the system evolves. We find that, if a halo is perturbed on small scales by a white noise-like force field induced by substructure (modeled as a perturbation external to the system considered), then a constant flux steady-state solution, corresponding to constant accretion, is the $\rho_0(r) \sim r^{-1}$ NFW cusp with $f_0(E) \sim (E - \Phi_c)^{-5/2}$ (Φ_c is the central halo potential). On the other hand, the zero flux steady-state solution that corresponds to an isolated halo is the trivial solution of an f_0 that is flat in energy. The corresponding density profile either has a central core like the Einasto profile or harbors an $r^{-1.5}$ prompt cusp, depending on the inner boundary condition. If a massive halo is accreting at a constant rate, then it tends to develop an r^{-1} density cusp; but, if the accretion stops, the inner density flattens out into an Einasto-like core, unless a massive compact subhalo or black hole resides at the center.

What drives the system towards these attractor states? It turns out that collective effects are crucial for the emergence of the r^{-1} NFW cusp. Without self-gravity, the particles would simply experience the bare perturbing potential and get directly heated by it. In the presence of self-gravity, however, the slower particles attract more neighbors, acquire higher effective mass and get less accelerated than in the absence of

self-gravity. This collective dressing becomes more important in the inner halo. It manifests in the monotonically decreasing functional dependence of the response matrix with angular momentum L_c, i.e., $\mathbb{M}_{pq} \sim L_c^{-2}$. Particles with lower angular momentum are more collectively dressed, and gain more inertia and less energy. In a homogeneous background, velocity swaps the role with angular momentum, i.e., lower velocity particles are less accelerated. As shown by [3], the same phenomenology of collective dressing applies in collisionless electrostatic plasmas, where slower particles attract more opposite charge and get more Debye-shielded. This reduces their effective charge and therefore their acceleration relative to the faster particles. In self-gravitating systems, collective dressing has the same effect of reducing the acceleration of the slower particles but by increasing their effective mass instead. The same inverse square nature of the electrostatic Coulomb force and the gravitational force ultimately gives rise to the universal v^{-2} dependence of the dielectric constant for forcing on scales larger than the Debye length in plasmas and the Jeans scale in self-gravitating systems. In an inhomogeneous galaxy/halo, this shows up in the L_c^{-2} dependence of the dielectric tensor. If the forcing acts like a white noise on super-Debye scales in an electrostatic plasma, then the universal nature of collective dressing results in a universal v^4 dependence of the diffusion coefficient and a v^{-5} (in 3D) DF as the constant flux steady state solution [3]. The same effect arises in an inhomogeneous halo due to substructure induced white noise perturbations on scales smaller than the radius r. The $(E - \Phi_c)^{-5/2} \sim v^{-5}$ DF corresponds to an r^{-1} density cusp, which shows that this profile is ultimately the result of collective collisionless relaxation. We do not obtain the outer r^{-3} fall-off of the NFW profile from our QLT formalism; whether this arises from a redness of the temporal fluctuations or any specific spatial dependence of the gravitational perturbations in the outer halo or in some other way is subject to future investigation. Recent high resolution cosmological N-body simulations [14] show that massive halos tend to develop an NFW cusp over long timescales, which suggests this process should be well described by a quasilinear formalism for collisionless relaxation, advocated in this paper.

Our approach towards modeling collisionless relaxation is similar to that of [15, 16], who solves the quasilinear diffusion equation to study the relaxation of halos perturbed by orbiting satellites. Contrary to our prediction, though, he only obtains an Einasto-like profile and not the r^{-1} NFW cusp as the end state. We believe that the following factors are responsible for this discrepancy: (1) due to computational complexity, he does not study the evolution of initially cuspy profiles that are produced by an initial phase of violent relaxation in cosmological simulations [14], and (2) he approximates the Fourier-Laplace coefficient of the total dressed potential, $\mathbf{A}$, in terms of that for the perturber potential, $\mathbf{b}$, as $\mathbf{A} = (\mathbb{I} + \mathbb{M})\,\mathbf{b}$, which is a linear order expansion in $\mathbb{M}$ of the full linear response equation (3), $\mathbf{A} = (\mathbb{I} - \mathbb{M})^{-1}\,\mathbf{b}$ [c.f. 32]. This approximation is only valid when the elements of the response matrix are small compared to unity. In the response theory for homogeneous systems, this corresponds to the dielectric constant being close to unity, representing the limit of weak polarization or weak collective effects, which occurs on scales smaller than or comparable to the Jeans scale. However, we show that the r^{-1} NFW cusp shows up when the collective dressing is strong, i.e., the elements of the response matrix significantly exceed unity.

The r^{-1} NFW cusp with a v^{-5} DF is an attractor steady state for halos that are accreting at a constant rate. An isolated halo, on the other hand, can approach a steady state with a flat energy distribution. The DF need not be flat throughout, rather it needs to be sufficiently shallow (log-slope tending to zero) at low velocities. The corresponding density profile can either harbor an Einasto-like core or an $r^{-1.5}$ prompt cusp. Both are possible end states of the broadening and flattening of the energy distribution via collisionless relaxation, as long as there is no net flux of material in the system. Unlike the NFW cusp, collective effects are not necessary to produce these profiles. Even if collective dressing prevails, collisionless relaxation eventually flattens the DF if there is no infall of matter. The prompt cusp requires the presence of a sufficiently compact object in the center, e.g., a massive compact subhalo or a black hole or such, in which case the (negative) potential Ψ_0 scales as $\sim r^{-1}$ farther out and the density scales as $\Psi_0^{3/2} \sim r^{-1.5}$. This reminds us of the secondary infall model of Bertschinger [18], which predicts the formation of an $r^{-1.5}$ cusp from the self-similar accretion of collisionless fluid onto a central black hole. Since N-body simulations model CDM as a collection of softened Plummer spheres, the formation of the smallest halos basically occurs via the assembly of several Plummer spheres around an equally massive central one, which satisfies the point mass-like inner boundary condition required for the emergence of an $r^{-1.5}$ density profile. More massive halos can also assume this profile if a massive compact subhalo inspirals all the way to the center under dynamical friction and yet survives tidal disruption (if the central density of the subhalo exceeds the background density of the halo). These are some potential reasons why recent high resolution N-body simulations predict $r^{-1.5}$ prompt cusps in the early phase of halo formation [14]. These simulations also predict that some of the massive halos attain an r^{-1} NFW-like outer cusp surrounding the inner prompt cusp in the latter stages of their lives. This is probably because, as the smaller halos accrete matter and grow in mass, collective collisionless relaxation induced by substructure drives the intermediate halo towards an r^{-1} cusp. The subtle dependence of the attractor states on the nature of the boundary conditions is a prediction of the present analytical model and can be tested by N-body simulations.

We have only looked for spherically symmetric and isotropic/ergodic steady state solutions to the quasilinear diffusion equation in this paper. There is, however, an entire landscape of distributions that satisfy the steady-state condition obtained by putting the RHS of equation (10) to zero, with the diffusion tensor and the response matrix respectively given by equations (11) and (12). This quasilinear condition reduces the enormous landscape of steady-state solutions allowed by the Vlasov equation to one with a much smaller measure. Instead of *any* positive definite function of the conserved quantities or actions as allowed by the Vlasov equation, now we have a *restricted* set of functions that follow the quasilinear

condition as the family of steady state solutions. On top of that, if we enforce spherical symmetry and velocity isotropy, then by the Doremus-Feix-Baumann Theorem and Antonov's Second Law we know that any such f_0 with $\mathrm{d}f_0/\mathrm{d}E < 0$ is linearly stable to all perturbations [37]. Therefore, all spherically symmetric and isotropic distributions that are monotonically decreasing in energy and satisfy the quasilinear steady state condition are steady-state attractors. Even though this landscape is much more restricted than that allowed by the Vlasov equation, it is still vast and largely unexplored. We have shown in this paper that the r^{-1} NFW cusp as well as a profile with a central core and an $r^{-1.5}$ prompt cusp are steady state attractors of the quasilinear diffusion equation. We have, however, only studied the relaxation of small I_r orbits in this paper since small-scale perturbations generally peak therein. This enables us to make scaling arguments and obtain a self-similar steady state solution with constant flux. We leave the more general but involved analysis including eccentric orbits and large-scale perturbations for future work.

Besides the spherical isotropic solutions we study here, there are many other steady state solutions to the quasilinear diffusion equation, ergodic or not. In particular, it would be interesting to see if the exponential profile that appears to be universal among disk galaxies emerges as an axisymmetric attractor of the quasilinear diffusion equation. We leave this for future investigation. In future work, we also intend to study the time-dependence of collisionless relaxation by integrating the quasilinear diffusion equation for realistic perturbations (sourced, for instance, by galaxy/halo impacts, or baryonic feedback), along the lines of Weinberg [15, 16] but including the full collective effects in the response matrix.

ACKNOWLEDGMENTS

The authors are thankful to the Kavli Institute of Theoretical Physics (KITP), University of California, Santa Barbara, where much of the manuscript was prepared, and to the organizers and attendees of the workshop, "Interconnections between the Physics of Plasmas and Self-gravitating Systems" at KITP, for insightful discussions. The authors are also thankful to Martin Weinberg, Toby Adkins, Frank van den Bosch, Pierre-Henri Chavanis, Robert Ewart, Jean-Baptiste Fouvry, Chris Hamilton, Matthew Kunz, Michael Nastac, Alex Schekochihin, Jonathan Squire, and Anna Lisa Varri for stimulating discussions and valuable suggestions. This research is supported by the National Science Foundation Award 2209471 at the Multi-Messenger Plasma Physics Center (MPPC), and Princeton University.

Appendix A: Linear response theory

The linearized Vlasov equation given by the first of equations (2) can be solved in the angle-action $(\mathbf{w}, \mathbf{I})$ space, in which case it reduces to

$$\frac{\partial f_1}{\partial t} + \mathbf{\Omega} \cdot \frac{\partial f_1}{\partial \mathbf{w}} = \frac{\partial f_0}{\partial \mathbf{I}} \cdot \frac{\partial H_1}{\partial \mathbf{w}}, \tag{A1}$$

where $\mathbf{\Omega} = (\Omega_1, \Omega_2, \Omega_3)$ (in 3D) are the frequencies, given by

$$\mathbf{\Omega} = \frac{\partial H_0}{\partial \mathbf{I}} \tag{A2}$$

It gets further simplified in the Fourier space of the angles. We expand f_1, Φ_1 and Φ_P as Fourier series in angles:

$$\begin{aligned} f_1(\mathbf{w}, \mathbf{I}, t) &= \sum_{\boldsymbol{\ell}} \exp\left[i\boldsymbol{\ell} \cdot \mathbf{w}\right] f_{1\boldsymbol{\ell}}(\mathbf{I}, t), \\ \Phi_1(\mathbf{w}, \mathbf{I}, t) &= \sum_{\boldsymbol{\ell}} \exp\left[i\boldsymbol{\ell} \cdot \mathbf{w}\right] \Phi_{1\boldsymbol{\ell}}(\mathbf{I}, t), \\ \Phi_\mathrm{P}(\mathbf{w}, \mathbf{I}, t) &= \sum_{\boldsymbol{\ell}} \exp\left[i\boldsymbol{\ell} \cdot \mathbf{w}\right] \Phi_{\boldsymbol{\ell}}(\mathbf{I}, t). \end{aligned} \tag{A3}$$

This reduces equation (A1) to the following evolution equation for $f_{1\boldsymbol{\ell}}$:

$$\frac{\partial f_{1\boldsymbol{\ell}}}{\partial t} + i\boldsymbol{\ell} \cdot \mathbf{\Omega} f_{1\boldsymbol{\ell}} = i\boldsymbol{\ell} \cdot \frac{\partial f_0}{\partial \mathbf{I}} \left(\Phi_{1\boldsymbol{\ell}} + \Phi_{\boldsymbol{\ell}}\right). \tag{A4}$$

Since we are interested in an initial value problem, we also take the Laplace transform in time:

$$\tilde{Q}(\mathbf{I}, \omega) = \int_0^\infty \mathrm{d}t \, \exp\left[i\omega t\right] Q(\mathbf{I}, t). \tag{A5}$$

This reduces equation (A4) to the following equation for $\tilde{f}_{1\boldsymbol{\ell}}(\mathbf{I}, \omega)$:

$$\tilde{f}_{1\boldsymbol{\ell}}(\mathbf{I}, \omega) = -\boldsymbol{\ell} \cdot \frac{\partial f_0}{\partial \mathbf{I}} \frac{\tilde{\Phi}_{1\boldsymbol{\ell}} + \tilde{\Phi}_{\boldsymbol{\ell}}}{\omega - \boldsymbol{\ell} \cdot \mathbf{\Omega}} - \frac{f_{1\boldsymbol{\ell}}(\mathbf{I}, 0)}{\omega - \boldsymbol{\ell} \cdot \mathbf{\Omega}}, \tag{A6}$$

with $f_{1\boldsymbol{\ell}}(\mathbf{I}, 0)$ the initial value of $f_{1\boldsymbol{\ell}}(\mathbf{I}, t)$.

Now, we need to relate $\Phi_{1\boldsymbol{\ell}}$ to $f_{1\boldsymbol{\ell}}$ through the Poisson equation. The gravitational potential, Φ, is related to the density, $\rho = \int \mathrm{d}^3 v f$ by

$$\Phi(\mathbf{x}) = \int \mathrm{d}^3 x' \, U(\mathbf{x}, \mathbf{x}') \rho(\mathbf{x}'), \tag{A7}$$

with the pairwise interaction potential, $U(\mathbf{x}, \mathbf{x}') = -G/|\mathbf{x} - \mathbf{x}'|$. This implies that $\tilde{\Phi}_{1\boldsymbol{\ell}}$ is related to $\tilde{f}_{1\boldsymbol{\ell}}$ as follows:

$$\tilde{\Phi}_{1\boldsymbol{\ell}}(\mathbf{I}) = (2\pi)^3 \sum_{\boldsymbol{\ell}'} \int \mathrm{d}\mathbf{I}' \Psi_{\boldsymbol{\ell}\boldsymbol{\ell}'}(\mathbf{I}, \mathbf{I}') \tilde{f}_{1\boldsymbol{\ell}'}(\mathbf{I}'), \tag{A8}$$

with

$$\begin{aligned} &\Psi_{\boldsymbol{\ell}\boldsymbol{\ell}'}(\mathbf{I}, \mathbf{I}') \\ &= \int \frac{\mathrm{d}^3 w}{(2\pi)^3} \int \frac{\mathrm{d}^3 w'}{(2\pi)^3} \, U(\mathbf{x}, \mathbf{x}') \, \exp\left[-i\left(\boldsymbol{\ell} \cdot \mathbf{w} + \boldsymbol{\ell}' \cdot \mathbf{w}'\right)\right]. \end{aligned} \tag{A9}$$

Combining equation (A8) with equation (A6), we can eliminate $\tilde{f}_{1\boldsymbol{\ell}}$ to obtain

$$\tilde{\Phi}_{1\boldsymbol{\ell}}(\mathbf{I}) = -(2\pi)^3 \sum_{\boldsymbol{\ell}'} \int \mathrm{d}\mathbf{I}'\, \boldsymbol{\ell}' \cdot \frac{\partial f_0}{\partial \mathbf{I}'} \frac{\Psi_{\boldsymbol{\ell}\boldsymbol{\ell}'}(\mathbf{I},\mathbf{I}')}{\omega - \boldsymbol{\ell}'\cdot\Omega'} \left[\tilde{\Phi}_{1\boldsymbol{\ell}'}(\mathbf{I}') + \tilde{\Phi}_{\boldsymbol{\ell}'}(\mathbf{I}')\right] + (2\pi)^3 i \sum_{\boldsymbol{\ell}'} \int \mathrm{d}\mathbf{I}' \frac{\Psi_{\boldsymbol{\ell}\boldsymbol{\ell}'}(\mathbf{I},\mathbf{I}')}{\omega - \boldsymbol{\ell}'\cdot\Omega'} f_{1\boldsymbol{\ell}'}(\mathbf{I}',0). \tag{A10}$$

This is an implicit equation for $\tilde{\Phi}_{1\boldsymbol{\ell}}$ and thus requires further simplification before a solution is attempted.

1. Bi-orthogonal basis method

A standard way to solve Equation (A10) is by expanding the potential and density in the bi-orthogonal basis $(\Psi^{(p)}, \rho^{(p)})$ that solve the Poisson equation [39]:

$$\Phi_1(\mathbf{x},t) = \sum_p a_p(t)\psi^{(p)}(\mathbf{x}), \quad \Phi_{\mathrm{P}}(\mathbf{x},t) = \sum_p b_p(t)\psi^{(p)}(\mathbf{x})$$
$$\rho_1(\mathbf{x},t) = \sum_p a_p(t)\rho^{(p)}(\mathbf{x}), \tag{A11}$$

such that

$$\psi^{(p)}(\mathbf{x}) = \int \mathrm{d}^3x'\, U(\mathbf{x},\mathbf{x}')\rho^{(p)}(\mathbf{x}'),$$
$$\int \mathrm{d}^3x\, \psi^{(p)*}(\mathbf{x})\rho^{(q)}(\mathbf{x}) = -4\pi G\, \delta_{pq}. \tag{A12}$$

In this basis, $\Psi_{\boldsymbol{\ell}\boldsymbol{\ell}'}(\mathbf{I},\mathbf{I}')$ reduces to

$$\Psi_{\boldsymbol{\ell}\boldsymbol{\ell}'}(\mathbf{I},\mathbf{I}') = -\frac{1}{4\pi G}\sum_p \psi^{(p)}_{\boldsymbol{\ell}}(\mathbf{I})\psi^{(p)*}_{\boldsymbol{\ell}'}(\mathbf{I}), \tag{A13}$$

where

$$\psi^{(p)}_{\boldsymbol{\ell}}(\mathbf{I}) = \frac{1}{(2\pi)^3}\int d^3w\, \psi^{(p)}(\mathbf{x}) \exp\left[-i\boldsymbol{\ell}\cdot\mathbf{w}\right]. \tag{A14}$$

In the bi-orthogonal basis, the implicit equation for $\tilde{\Phi}_{1\boldsymbol{\ell}}$ given by equation (A10) reduces to the following matrix equation:

$$\tilde{\mathbf{a}}(\omega) = (\mathbb{I} - \mathbb{M}(\omega))^{-1}\left(\mathbf{s}(\omega) + \mathbb{M}(\omega)\,\tilde{\mathbf{b}}(\omega)\right), \tag{A15}$$

where $\tilde{\mathbf{a}} = \{a_1, a_2, ...\}$ is the response vector and $\tilde{\mathbf{b}} = \{b_1, b_2, ...\}$ is the perturbation vector. The response matrix $\mathbb{M}$ is given by

$$\mathbb{M}_{pq}(\omega) = \frac{(2\pi)^3}{4\pi G}\sum_{\boldsymbol{\ell}}\int \mathrm{d}\mathbf{I}\, \boldsymbol{\ell}\cdot\frac{\partial f_0}{\partial \mathbf{I}}\frac{\psi^{(p)*}_{\boldsymbol{\ell}}(\mathbf{I})\psi^{(q)}_{\boldsymbol{\ell}}(\mathbf{I})}{\omega - \boldsymbol{\ell}\cdot\Omega}. \tag{A16}$$

The vector corresponding to the initial DF perturbation is given by

$$\mathbf{s}_p(\omega) = (2\pi)^3 i \sum_{\boldsymbol{\ell}}\int \mathrm{d}\mathbf{I}\, \frac{f_{1\boldsymbol{\ell}}(\mathbf{I},0)}{\omega - \boldsymbol{\ell}\cdot\Omega}\,\psi^{(p)*}_{\boldsymbol{\ell}}(\mathbf{I}). \tag{A17}$$

Note that this assumes the unit of $\psi^{(p)}_{\boldsymbol{\ell}}$ to be $G/\sqrt{|\mathbf{x}|}$ and that of a_p or b_p to be $M/\sqrt{|\mathbf{x}|}$ (M is mass).

2. Temporal response

The temporal response can be obtained by taking the inverse Laplace transform of equation (A15):

$$\mathbf{a}(t) = \frac{1}{2\pi}\int_{ic-\infty}^{ic+\infty} \mathrm{d}\omega\, \exp\left[-i\omega t\right]\tilde{\mathbf{a}}(\omega)$$
$$= \frac{1}{2\pi}\int_{ic-\infty}^{ic+\infty} \mathrm{d}\omega\, \exp\left[-i\omega t\right]$$
$$\times \left[\mathbb{I} - \mathbb{M}(\omega)\right]^{-1}\left[\mathbf{s}(\omega) + \mathbb{M}(\omega)\,\tilde{\mathbf{b}}(\omega)\right], \tag{A18}$$

where c is chosen such that the integration contour lies in the region of convergence of $\tilde{\mathbf{a}}$. Typically, this means that c exceeds the maximum of the real parts of the poles of $\tilde{a}_p$. The contribution to the inverse Laplace transform comes from the poles of $\tilde{\mathbf{a}}$, i.e., the poles of $\tilde{\mathbf{b}}$, $\omega = \boldsymbol{\ell}\cdot\Omega$, and the values of ω such that

$$\det\left[\mathbb{I} - \mathbb{M}(\omega)\right] = 0. \tag{A19}$$

The discrete values of ω, ω_n, which follow this dispersion relation correspond to the self-sustaining oscillations of the system, known as point modes. All the point modes of a stable self-gravitating system are damped, i.e., have $\mathrm{Re}(\omega_n) < 0$. This phenomenon is known as Landau damping. In an unstable system, one or more of the point modes grows ($\mathrm{Re}(\omega_n) > 0$). When a system is marginally stable, the real part of one of the modes sits very close to zero, while all other modes are heavily damped.

The coefficient of the total potential is equal to $\tilde{\mathbf{a}} + \tilde{\mathbf{b}} = (\mathbb{I} - \mathbb{M})^{-1}\tilde{\mathbf{b}}$ (assuming that $f_{1\boldsymbol{\ell}}(\mathbf{I},0) = 0$, i.e., $\mathbf{s} = 0$). For simplicity, $\mathbf{b}(t)$ can be expanded as the following Fourier series:

$$\mathbf{b}(t) = \int \mathrm{d}\omega^{(\mathrm{P})} \exp\left[-i\omega^{(\mathrm{P})}t\right]\mathbf{b}\left(\omega^{(\mathrm{P})}\right), \tag{A20}$$

which can be Laplace transformed to yield

$$\tilde{\mathbf{b}}(\omega) = i\int \mathrm{d}\omega^{(\mathrm{P})}\,\frac{\mathbf{b}\left(\omega^{(\mathrm{P})}\right)}{\omega - \omega^{(\mathrm{P})}}. \tag{A21}$$

Now, upon performing the inverse Laplace transform of $\mathbf{a}+\mathbf{b}$, we obtain the following temporal dependence for the Fourier mode of the total potential (including the perturber potential and the linear response):

$$\Phi_{\boldsymbol{\ell}}(\mathbf{I},t) = \Phi_{\mathrm{P}\boldsymbol{\ell}}(\mathbf{I},t) + \Phi_{1\boldsymbol{\ell}}(\mathbf{I},t) = \left(a_p(t)+b_p(t)\right)\psi^{(p)}_{\boldsymbol{\ell}}(\mathbf{I}) = \int \mathrm{d}\omega^{(\mathrm{P})} \exp\left[-i\omega^{(\mathrm{P})}t\right]\left[\mathbb{I}-\mathbb{M}\left(\omega^{(\mathrm{P})}\right)\right]^{-1}_{pq} b_q\left(\omega^{(\mathrm{P})}\right)\psi^{(p)}_{\boldsymbol{\ell}}(\mathbf{I}), \tag{A22}$$

where we have taken the long time limit, i.e., evaluated the response at times longer than the damping time of the least damped Landau mode, assuming that the system is linearly stable.

The linear response in the DF can be obtained by taking the inverse Laplace transform of $f_{1\boldsymbol{\ell}}$ from equation (A6):

$$f_{1\boldsymbol{\ell}}(\mathbf{I},t) = -\boldsymbol{\ell}\cdot\frac{\partial f_0}{\partial \mathbf{I}}\int \mathrm{d}\omega^{(\mathrm{P})}\frac{b_q\left(\omega^{(\mathrm{P})}\right)\psi^{(p)}_{\boldsymbol{\ell}}(\mathbf{I})}{\omega^{(\mathrm{P})}-\boldsymbol{\ell}\cdot\boldsymbol{\Omega}}\left[\left(\mathbb{I}-\mathbb{M}\left(\omega^{(\mathrm{P})}\right)\right)^{-1}_{pq}\exp\left[-i\omega^{(\mathrm{P})}t\right] - \left(\mathbb{I}-\mathbb{M}\left(\boldsymbol{\ell}\cdot\boldsymbol{\Omega}\right)\right)^{-1}_{pq}\exp\left[-i\boldsymbol{\ell}\cdot\boldsymbol{\Omega}t\right]\right]. \tag{A23}$$

The response thus consists of a term that follows the temporal dependence of the perturber and another that oscillates at the unperturbed frequencies but is dressed by collective interactions.

The evolution of the phase-averaged DF, $\int \mathrm{d}^3w\, f_2/(2\pi)^3 = f_{2\boldsymbol{\ell}\to 0} = f_0$, is obtained by putting $\boldsymbol{\ell}=0$ in the above equation, and is given by the following quasilinear equation:

$$\frac{\partial f_0}{\partial t} = i\sum_{\boldsymbol{\ell}}\boldsymbol{\ell}\cdot\frac{\partial}{\partial \mathbf{I}}\left\langle f^*_{1\boldsymbol{\ell}}(\mathbf{I},t)\,\Phi_{\boldsymbol{\ell}}(\mathbf{I},t)\right\rangle, \tag{B2}$$

where we have defined $\Phi_{\boldsymbol{\ell}} = \Phi_{\mathrm{P}\boldsymbol{\ell}} + \Phi_{1\boldsymbol{\ell}}$, and used the reality condition that $f_{1,-\boldsymbol{\ell}} = f^*_{1\boldsymbol{\ell}}$. The brackets $\langle Q\rangle$ denote the ensemble average of the quantity Q over random phases.

Now we assume that the perturber potential assumes the following form of a red noise:

$$\left\langle b^*_q(t)\, b_{q'}(t')\right\rangle = B^*_q B_{q'} C_t(t-t'), \tag{B3}$$

where C_t denotes the temporal correlation function, which is equal to $\delta(t-t')$ for white/uncorrelated noise. Therefore, the Fourier transform of $b_q(t)$, $b_q\left(\omega^{(\mathrm{P})}\right)$, follows the condition:

$$\left\langle b^*_q\left(\omega^{(\mathrm{P})}\right) b_{q'}\left(\omega^{(\mathrm{P})}\right)\right\rangle = \frac{1}{(2\pi)^2}\int \mathrm{d}t\int \mathrm{d}t' \exp\left[i\left(\omega^{(\mathrm{P})}t - \omega'^{(\mathrm{P})}t'\right)\right]\left\langle b^*_q(t)\, b_{q'}(t')\right\rangle = B^*_q B_{q'} C_\omega\left(\omega^{(\mathrm{P})}\right)\delta\left(\omega^{(\mathrm{P})}-\omega'^{(\mathrm{P})}\right), \tag{B4}$$

where C_ω denotes the Fourier transform of C_t.

Substituting the linear responses from equations (A23) and (A22) in the quasilinear equation (B2), we obtain

Appendix B: Quasilinear response theory

Linear response theory describes the evolution of the fluctuations on top of a smooth background, but the background itself evolves due to the combined action of the linear fluctuations. Modeling this requires performing a second order or quasilinear perturbation of the Vlasov-Poisson equations. The second order response equation for the Fourier transform of f_2 is given by

$$\frac{\partial f_{2\boldsymbol{\ell}}}{\partial t} + i\boldsymbol{\ell}\cdot\boldsymbol{\Omega} f_{2\boldsymbol{\ell}} = i\boldsymbol{\ell}\cdot\frac{\partial f_0}{\partial \mathbf{I}}\Phi_{2\boldsymbol{\ell}} + i\sum_{\boldsymbol{\ell}'}\left[\boldsymbol{\ell}'\cdot\frac{\partial f_{1\boldsymbol{\ell}-\boldsymbol{\ell}'}}{\partial \mathbf{I}}\left(\Phi_{1\boldsymbol{\ell}'}+\Phi_{\boldsymbol{\ell}'}\right) - (\boldsymbol{\ell}-\boldsymbol{\ell}')\cdot\frac{\partial\left(\Phi_{1\boldsymbol{\ell}'}+\Phi_{\boldsymbol{\ell}'}\right)}{\partial \mathbf{I}} f_{1\boldsymbol{\ell}-\boldsymbol{\ell}'}\right]. \tag{B1}$$

$$\frac{\partial f_0}{\partial t} = \sum_{\boldsymbol{\ell}} \boldsymbol{\ell} \cdot \frac{\partial}{\partial \mathbf{I}} \left(D_{\boldsymbol{\ell}} (\mathbf{I}, t)\, \boldsymbol{\ell} \cdot \frac{\partial f_0}{\partial \mathbf{I}} \right), \tag{B5}$$

where $D_{\boldsymbol{\ell}} (\mathbf{I}, t)$ is given by

$$\begin{aligned} D_{\boldsymbol{\ell}} (\mathbf{I}, t) = -i \int \mathrm{d}\omega^{(\mathrm{P})}\, C_{\omega} \left(\omega^{(\mathrm{P})}\right) \frac{B_q^* \left(\omega^{(\mathrm{P})}\right) B_{q'} \left(\omega^{(\mathrm{P})}\right) \psi_{\boldsymbol{\ell}}^{(p)*} \psi_{\boldsymbol{\ell}}^{(p')}}{\omega^{(\mathrm{P})} - \boldsymbol{\ell} \cdot \boldsymbol{\Omega}} \left(\mathbb{I} - \mathbb{M} \left(\omega^{(\mathrm{P})}\right)\right)^{-1}_{pq} \\ \times \left[\left(\mathbb{I} - \mathbb{M}^* \left(\omega^{(\mathrm{P})}\right)\right)^{-1}_{p'q'} - \left(\mathbb{I} - \mathbb{M}^* \left(\boldsymbol{\ell} \cdot \boldsymbol{\Omega}\right)\right)^{-1}_{p'q'} \exp\left[-i \left(\omega^{(\mathrm{P})} - \boldsymbol{\ell} \cdot \boldsymbol{\Omega}\right) t\right] \right]. \end{aligned} \tag{B6}$$

In the long time limit, which is what we are interested in, $D_{\boldsymbol{\ell}} (\mathbf{I}, t)$ reduces to

$$\begin{aligned} &\lim_{t \to \infty} D_{\boldsymbol{\ell}} (\mathbf{I}, t) = D_{\boldsymbol{\ell}} (\mathbf{I}) \\ &= \left| \left(\mathbb{I} - \mathbb{M} \left(\boldsymbol{\ell} \cdot \boldsymbol{\Omega}\right)\right)^{-1}_{pq} B_q \psi_{\boldsymbol{\ell}}^{(p)} (\mathbf{I}) \right|^2 C_{\omega} \left(\boldsymbol{\ell} \cdot \boldsymbol{\Omega}\right). \end{aligned} \tag{B7}$$

Here we have used the identity that $\lim_{t \to \infty} \exp\left[-ixt\right]/x = 1/x - i\pi\delta\left(x\right)$ with $x = \omega^{(\mathrm{P})} - \boldsymbol{\ell} \cdot \boldsymbol{\Omega}$.

Appendix C: Computing the Fourier coefficients of basis functions

A natural set of orthogonal basis functions that describes spherically symmetric potential perturbations in a spherical galaxy/halo is given by

$$\psi^{(p)}(r) = -\frac{G M_{\mathrm{h}}}{r} \exp\left[ipk_r r\right], \tag{C1}$$

with k_r a characteristic radial wavenumber and M_{h} a characteristic mass. The corresponding Fourier coefficient, $\psi_{\boldsymbol{\ell}}^{(p)} (\mathbf{I})$, typically peaks at small I_r (as we show below). Therefore we can adopt the radial epicyclic approximation to compute it, i.e., assume [37]

$$\begin{aligned} r &\approx R_{\mathrm{c}}(L) + \sqrt{\frac{2I_r}{\kappa}} \sin w_r, \\ \phi &\approx w_\phi + \frac{2\Omega_\phi}{R_{\mathrm{c}}\kappa} \sqrt{\frac{2I_r}{\kappa}} \cos w_r, \end{aligned} \tag{C2}$$

with $\boldsymbol{\ell} = \left(\ell_r, \ell_\phi\right)$, L the angular momentum, $R_{\mathrm{c}}(L)$ the guiding radius, I_r the radial action, Ω_ϕ the azimuthal frequency on the orbital plane, $\kappa = \Omega_r(L, I_r = 0)$ the radial epicyclic frequency, w_ϕ the azimuthal angle and w_r the radial angle. The Fourier coefficient can thus be computed as follows:

$$\psi_{\boldsymbol{\ell}}^{(p)} (\mathbf{I}) \approx -\frac{G M_{\mathrm{h}}}{2\pi} \exp\left[ipk_r R_{\mathrm{c}}\right] \int_0^{2\pi} \mathrm{d}w_r \frac{\exp\left[i\left(pk_r \sqrt{\frac{2I_r}{\kappa}} \sin w_r + \frac{2\ell_\phi \Omega_\phi}{R_{\mathrm{c}}\kappa} \sqrt{\frac{2I_r}{\kappa}} \cos w_r - \ell_r w_r\right)\right]}{R_{\mathrm{c}}\left(L\right) + \sqrt{\frac{2I_r}{\kappa}} \sin w_r}, \tag{C3}$$

which simplifies into the following:

$$\psi_{\boldsymbol{\ell}}^{(p)} (\mathbf{I}) \approx -\frac{G M_{\mathrm{h}}}{2\pi} \frac{\exp\left[ipk_r R_{\mathrm{c}}\right]}{R_{\mathrm{c}}} \int_0^{2\pi} \mathrm{d}w_r \frac{\exp\left[i\left(pb \sin w_r + 2\ell_\phi \gamma a \cos w_r - \ell_r w_r\right)\right]}{1 + a \sin w_r}, \tag{C4}$$

with $a = r_0/R_{\mathrm{c}}$, $b = k_r r_0$, $r_0 = \sqrt{2I_r/\kappa}$ and $\gamma = \Omega_\phi/\kappa$. Note that the epicyclic approximation is only valid for $r_0 \lesssim R_{\mathrm{c}}$ or

$a \lesssim 1$. In this case, $(1 + a \sin w_r)^{-1}$ can be expanded as a binomial series in $a \sin w_r$, and the above integral can be analytically evaluated to yield the following series expansion for $\psi^{(p)}_{\boldsymbol{\ell}}$:

$$\psi^{(p)}_{\boldsymbol{\ell}}(\mathbf{I}) \approx -\frac{GM_{\rm h}}{R_{\rm c}} \exp\left[ipk_r R_{\rm c}\right] \sum_{n=0}^{\infty} (-i)^n \left(\frac{a}{p}\right)^n \frac{\partial^n}{\partial b^n} \left[\exp\left[i\ell \tan^{-1}\left(\frac{2\ell_\phi \gamma a}{pb}\right) J_{\ell_r}\left(\sqrt{4\ell_\phi^2\gamma^2 a^2 + p^2 b^2}\right)\right]\right], \tag{C5}$$

where J_{ℓ_r} denotes the $\ell_r^{\rm th}$ order Bessel function of the first kind. Here we have used the identity that $\int_0^{2\pi} {\rm d}\theta \exp\left[i\left(A\sin\theta - \ell\theta\right)\right] = 2\pi J_\ell(A)$. For $r_0 \ll R_{\rm c}$, i.e., $a \ll 1$, we can further approximate the above expression as

$$\begin{aligned}\psi^{(p)}_{\boldsymbol{\ell}}(\mathbf{I}) \approx -\frac{GM_{\rm h}}{R_{\rm c}} \exp\left[i\left(pk_r R_{\rm c} + \tan^{-1}\left(\frac{2\ell_\phi\gamma}{pk_r R_{\rm c}}\right)\right)\right] \\ \times \left[\left(1 + \frac{2\ell_\phi\gamma}{4\ell_\phi^2\gamma^2 + p^2 k_r^2 R_{\rm c}^2}\right) J_{\ell_r}\left(k_r r_0 \sqrt{\frac{4\ell_\phi^2\gamma^2}{k_r^2 R_{\rm c}^2} + p^2}\right) - \frac{ir_0}{R_{\rm c}} \frac{1}{\sqrt{1 + \frac{4\ell_\phi^2\gamma^2}{p^2 k_r^2 R_{\rm c}^2}}} J'_{\ell_r}\left(k_r r_0 \sqrt{\frac{4\ell_\phi^2\gamma^2}{k_r^2 R_{\rm c}^2} + p^2}\right)\right].\end{aligned} \tag{C6}$$

It is not hard to see that most of the contribution comes from small r_0 and therefore small I_r, for both small and large $k_r R_{\rm c}$. This validates our radial epicyclic approximation in the evaluation of the Fourier coefficients to begin with.

1. Large $k_r R_{\rm c}$

The response matrix and the reduced diffusion coefficient (equation [18]) involves the factor $\psi^{p*}_{\boldsymbol{\ell}} \psi^{q}_{\boldsymbol{\ell}}$ which when integrated over I_r yields the following for $k_r R_{\rm c} \gg 1$:

$$\begin{aligned}\int_0^\infty {\rm d}I_r\, \psi^{p*}_{\boldsymbol{\ell}}(\mathbf{I}) \psi^{q}_{\boldsymbol{\ell}}(\mathbf{I}) &\sim \frac{\kappa}{k_r^2} \frac{\exp\left[-i\left(p-q\right)k_r R_{\rm c}\right]}{R_{\rm c}^2} \\ &\times \left(1 + \frac{2\ell_\phi\gamma}{4\ell_\phi^2\gamma^2 + p^2 k_r^2 R_{\rm c}^2}\right)\left(1 + \frac{2\ell_\phi\gamma}{4\ell_\phi^2\gamma^2 + q^2 k_r^2 R_{\rm c}^2}\right) \int_0^{k_r R_{\rm c}} {\rm d}z\, z\, J_{\ell_r}\left(z\sqrt{\frac{4\ell_\phi^2\gamma^2}{k_r^2 R_{\rm c}^2} + p^2}\right) J_{\ell_r}\left(z\sqrt{\frac{4\ell_\phi^2\gamma^2}{k_r^2 R_{\rm c}^2} + q^2}\right) \\ &\approx \frac{\kappa}{k_r^2} \frac{\exp\left[-i\left(p-q\right)k_r R_{\rm c}\right]}{R_{\rm c}^2} \frac{\delta\left(\sqrt{\frac{4\ell_\phi^2\gamma^2}{k_r^2 R_{\rm c}^2} + p^2} - \sqrt{\frac{4\ell_\phi^2\gamma^2}{k_r^2 R_{\rm c}^2} + q^2}\right)}{\sqrt{\frac{4\ell_\phi^2\gamma^2}{k_r^2 R_{\rm c}^2} + p^2}} \\ &\approx \frac{\kappa}{k_r^2 R_{\rm c}^2} \frac{\delta\left(p-q\right)}{p}.\end{aligned} \tag{C7}$$

Here we have used the identity that $\int_0^\infty {\rm d}z\, z\, J_\ell(uz) J_\ell(vz) = \delta\left(u-v\right)/u$. Only the first term in the series expansion of $\psi^{(p)}_{\boldsymbol{\ell}}$ survives, and only the diagonal terms of $\mathbb{M}_{pq}$ are non-zero in the large $k_r R_{\rm c}$ (WKB) limit.

2. Small $k_r R_c$

For small $k_r R_c$, the integral $\int_0^\infty \mathrm{d}I_r\, \psi_{\boldsymbol{\ell}}^{p*}(\mathbf{I})\psi_{\boldsymbol{\ell}}^{q}(\mathbf{I})$ can be evaluated as follows:

$$\int_0^\infty \mathrm{d}I_r\, \psi_{\boldsymbol{\ell}}^{p*}(\mathbf{I})\psi_{\boldsymbol{\ell}}^{q}(\mathbf{I}) \sim \frac{\kappa}{k_r^2}\frac{\exp\left[-i\,(p-q)\,k_r R_c\right]}{R_c^2}\mathcal{I}_{pq}(\ell_r, \ell_\phi, k_r, R_c) \tag{C8}$$

with

$$\begin{aligned}\mathcal{I}_{pq}(\ell_r, \ell_\phi, k_r, R_c) &= \left(1+\frac{2\ell_\phi\gamma}{4\ell_\phi^2\gamma^2+p^2k_r^2R_c^2}\right)\left(1+\frac{2\ell_\phi\gamma}{4\ell_\phi^2\gamma^2+q^2k_r^2R_c^2}\right) I\,(\alpha,\beta,\ell_r,k_rR_c)\\ &+\frac{i}{k_rR_c}\left(\frac{1}{\sqrt{1+\dfrac{4\ell_\phi^2\gamma^2}{q^2k_r^2R_c^2}}}\left(1+\frac{2\ell_\phi\gamma}{4\ell_\phi^2\gamma^2+p^2k_r^2R_c^2}\right)\frac{\partial}{\partial\beta}I\,(\alpha,\beta,\ell_r,k_rR_c) - \frac{1}{\sqrt{1+\dfrac{4\ell_\phi^2\gamma^2}{p^2k_r^2R_c^2}}}\left(1+\frac{2\ell_\phi\gamma}{4\ell_\phi^2\gamma^2+q^2k_r^2R_c^2}\right)\frac{\partial}{\partial\alpha}I\,(\alpha,\beta,\ell_r,k_rR_c)\right)\\ &+\frac{1}{k_r^2R_c^2}\frac{1}{\sqrt{\left(1+\dfrac{4\ell_\phi^2\gamma^2}{p^2k_r^2R_c^2}\right)\left(1+\dfrac{4\ell_\phi^2\gamma^2}{q^2k_r^2R_c^2}\right)}}\frac{\partial^2}{\partial\alpha\partial\beta}I\,(\alpha,\beta,\ell_r,k_rR_c)\,,\end{aligned} \tag{C9}$$

where $\alpha = \sqrt{\dfrac{4\ell_\phi^2\gamma^2}{k_r^2R_c^2}+p^2}$, $\beta = \sqrt{\dfrac{4\ell_\phi^2\gamma^2}{k_r^2R_c^2}+q^2}$, and $I\,(\alpha,\beta,\ell_r,k_rR_c)$ is given by

$$I\,(\alpha,\beta,\ell_r,k_rR_c) = \int_0^{k_rR_c}\mathrm{d}z\, z\, J_{\ell_r}(\alpha z)J_{\ell_r}(\beta z). \tag{C10}$$

$\mathcal{I}_{pq}$ scales differently with k_rR_c in two different regimes. If $\ell_\phi \gtrsim pk_rR_c/2\gamma$ and $\ell_\phi \gtrsim qk_rR_c/2\gamma$, then we have $\alpha=\beta\approx 2\ell_\phi\gamma/k_rR_c$, which implies

$$\begin{aligned} I &= \left(\frac{k_rR_c}{2\ell_\phi\gamma}\right)^2\int_0^{2\ell_\phi\gamma}\mathrm{d}z\, z\, J_{\ell_r}^2(z),\\ \frac{\partial I}{\partial\alpha} &= \frac{\partial I}{\partial\beta} = \left(\frac{k_rR_c}{2\ell_\phi\gamma}\right)^3\left[\left(2\ell_\phi\gamma\right)^2J_{\ell_r}^2\left(2\ell_\phi\gamma\right)-2I\right],\\ \frac{\partial^2 I}{\partial\alpha\partial\beta} &= \left(\frac{k_rR_c}{2\ell_\phi\gamma}\right)^4\left[6I-5\left(2\ell_\phi\gamma\right)^2J_{\ell_r}^2\left(2\ell_\phi\gamma\right)\right.\\ &\left.+2\left(2\ell_\phi\gamma\right)^3J_{\ell_r}\left(2\ell_\phi\gamma\right)J'_{\ell_r}\left(2\ell_\phi\gamma\right)\right]. \end{aligned} \tag{C11}$$

Since $2\ell_\phi\gamma \gtrsim pk_rR_c$, $2\ell_\phi\gamma \gtrsim qk_rR_c$ and $\partial I/\partial\alpha = \partial I/\partial\beta$ in this regime, we see that the second term of $\mathcal{I}_{pq}$ vanishes. And, since $k_rR_c/2\ell_\phi\gamma < 1/p < 1$ and $k_rR_c/2\ell_\phi\gamma < 1/q < 1$, the third term is smaller than the first by order $\sim \left(k_rR_c/2\ell_\phi\gamma\right)^4$. Therefore, $\int_0^\infty \mathrm{d}I_r\, \psi_{\boldsymbol{\ell}}^{p*}(\mathbf{I})\psi_{\boldsymbol{\ell}}^{q}(\mathbf{I})$ reduces to

$$\int_0^\infty \mathrm{d}I_r\, \psi_{\boldsymbol{\ell}}^{p*}(\mathbf{I})\psi_{\boldsymbol{\ell}}^{q}(\mathbf{I}) \sim \frac{\kappa}{4\ell_\phi^2\gamma^2}\left(1+\frac{1}{2\ell_\phi\gamma}\right)^2\exp\left[-i\,(p-q)\,k_rR_c\right]\int_0^{2\ell_\phi\gamma}\mathrm{d}z\, z\, J_{\ell_r}^2(z). \tag{C12}$$

On the other hand, if $\ell_\phi \lesssim pk_rR_c/2\gamma$ and $\ell_\phi \lesssim qk_rR_c/2\gamma$, then we have $\alpha \approx p$ and $\beta \approx q$, which implies that for $pk_rR_c \gtrsim 1$ and $qk_rR_c \gtrsim 1$,

$$\begin{aligned} I &= \frac{\delta(p-q)}{p}, \\ \frac{\partial I}{\partial \alpha} &= \frac{\partial I}{\partial \beta} = -\frac{\delta(p-q)}{p^2}, \\ \frac{\partial^2 I}{\partial \alpha \partial \beta} &= \frac{2\,\delta(p-q)}{p^3}. \end{aligned} \tag{C13}$$

Therefore, we see that the second term of $\mathcal{I}_{pq}$ vanishes again, while the third term is smaller than the first by order $(pk_rR_c)^2$. This yields

$$\int_0^\infty \mathrm{d}I_r\, \psi_{\boldsymbol{\ell}}^{p*}(\mathbf{I})\psi_{\boldsymbol{\ell}}^{q}(\mathbf{I}) \sim \frac{\kappa}{k_r^2 R_c^2}\frac{\delta(p-q)}{p}. \tag{C14}$$

Hence, we obtain the same scaling with R_c as in the WKB limit ($k_rR_c \gg 1$). This is expected since large p and q imply small scales just as $k_rR_c \gg 1$ does. In other words, large p and q also imply the WKB limit. We see that for each $p \gtrsim 1/k_rR_c$ and $q \gtrsim 1/k_rR_c$, the $l_\phi \lesssim pk_rR_c/2\gamma$ and $l_\phi \lesssim qk_rR_c/2\gamma$ terms of $\int_0^\infty \mathrm{d}I_r\, \psi_{\boldsymbol{\ell}}^{p*}(\mathbf{I})\psi_{\boldsymbol{\ell}}^{q}(\mathbf{I})$ dominate over the $l_\phi \gtrsim pk_rR_c/2\gamma$ and $l_\phi \gtrsim qk_rR_c/2\gamma$ terms by a factor of $(k_rR_c)^{-2}$ since $k_rR_c \lesssim 1$. Therefore, all $p \gtrsim 1/k_rR_c$ and $q \gtrsim 1/k_rR_c$ terms scale as $(k_rR_c)^{-2}$ for $k_rR_c \lesssim 1$. The $pk_rR_c \lesssim 1$ and $qk_rR_c \lesssim 1$ terms are much smaller and can be found to scale similarly as equation (C12).

From the above analysis, it is evident that for small as well as large k_rR_c, the diagonal elements of the response matrix are the dominant ones. For small k_rR_c, the elements with $pk_rR_c = qk_rR_c \gtrsim 1$ dominate.

[1] D. Lynden-Bell, Statistical mechanics of violent relaxation in stellar systems, MNRAS **136**, 101 (1967).

[2] R. J. Ewart, A. Brown, T. Adkins, and A. A. Schekochihin, Collisionless relaxation of a Lynden-Bell plasma, Journal of Plasma Physics **88**, 925880501 (2022), arXiv:2201.03376 [physics.plasm-ph].

[3] U. Banik, A. Bhattacharjee, and W. Sengupta, Universal non-thermal power-law distribution functions from the self-consistent evolution of collisionless electrostatic plasmas, arXiv e-prints , arXiv:2408.07127 (2024), arXiv:2408.07127 [astro-ph.SR].

[4] P. H. Chavanis, Kinetic theory of spatially homogeneous systems with long-range interactions: I. General results, European Physical Journal Plus **127**, 19 (2012), arXiv:1112.0772 [cond-mat.stat-mech].

[5] P.-H. Chavanis, Kinetic theory of collisionless relaxation for systems with long-range interactions, Physica A Statistical Mechanics and its Applications **606**, 128089 (2022), arXiv:2112.13664 [cond-mat.stat-mech].

[6] P.-H. Chavanis, The Secular Dressed Diffusion Equation, Universe **9**, 68 (2023).

[7] C. Hamilton and J.-B. Fouvry, Kinetic Theory of Stellar Systems: A Tutorial, arXiv e-prints , arXiv:2402.13322 (2024), arXiv:2402.13322 [astro-ph.GA].

[8] J. F. Navarro, C. S. Frenk, and S. D. M. White, A Universal Density Profile from Hierarchical Clustering, Astrophys. J. **490**, 493 (1997), astro-ph/9611107.

[9] B. Moore, F. Governato, T. Quinn, J. Stadel, and G. Lake, Resolving the Structure of Cold Dark Matter Halos, ApJL **499**, L5 (1998), astro-ph/9709051.

[10] J. F. Navarro, E. Hayashi, C. Power, A. R. Jenkins, C. S. Frenk, S. D. M. White, V. Springel, J. Stadel, and T. R. Quinn, The inner structure of ΛCDM haloes - III. Universality and asymptotic slopes, MNRAS **349**, 1039 (2004), arXiv:astro-ph/0311231 [astro-ph].

[11] J. F. Navarro, A. Ludlow, V. Springel, J. Wang, M. Vogelsberger, S. D. M. White, A. Jenkins, C. S. Frenk, and A. Helmi, The diversity and similarity of simulated cold dark matter haloes, MNRAS **402**, 21 (2010), arXiv:0810.1522 [astro-ph].

[12] J. Diemand, M. Kuhlen, and P. Madau, Formation and Evolution of Galaxy Dark Matter Halos and Their Substructure, Astrophys. J. **667**, 859 (2007), astro-ph/0703337.

[13] J. Einasto, On the Construction of a Composite Model for the Galaxy and on the Determination of the System of Galactic Parameters, Trudy Astrofizicheskogo Instituta Alma-Ata **5**, 87 (1965).

[14] M. S. Delos and S. D. M. White, Inner cusps of the first dark matter haloes: formation and survival in a cosmological context, MNRAS **518**, 3509 (2023), arXiv:2207.05082 [astro-ph.CO].

[15] M. D. Weinberg, Noise-driven evolution in stellar systems - II. A universal halo profile, MNRAS **328**, 321 (2001), arXiv:astro-ph/0007276 [astro-ph].

[16] M. D. Weinberg, Noise-driven evolution in stellar systems - I. Theory, MNRAS **328**, 311 (2001), arXiv:astro-ph/0007275 [astro-ph].

[17] J. A. Fillmore and P. Goldreich, Self-similar gravitational collapse in an expanding universe, Astrophys. J. **281**, 1 (1984).

[18] E. Bertschinger, Self-similar secondary infall and accretion in an Einstein-de Sitter universe, ApJS **58**, 39 (1985).

[19] V. A. Antonov, On the instability of stationary spherical models with merely radial motions., in *Dynamics of Galaxies and Star Clusters*, edited by T. B. Omarov (1973) pp. 139–143.

[20] A. Nusser, Self-similar spherical collapse with non-radial motions, MNRAS **325**, 1397 (2001), arXiv:astro-ph/0008217 [astro-ph].

[21] Y. Lu, H. J. Mo, N. Katz, and M. D. Weinberg, On the origin of cold dark matter halo density profiles, MNRAS **368**, 1931 (2006), arXiv:astro-ph/0508624 [astro-ph].

[22] A. Dekel, J. Devor, and G. Hetzroni, Galactic halo cusp-core: tidal compression in mergers, MNRAS **341**, 326 (2003), astro-ph/0204452.

[23] A. Dekel, I. Arad, J. Devor, and Y. Birnboim, Dark Halo Cusp: Asymptotic Convergence, Astrophys. J. **588**, 680 (2003), arXiv:astro-ph/0205448 [astro-ph].

[24] U. Banik and F. C. van den Bosch, A Self-consistent, Time-

dependent Treatment of Dynamical Friction: New Insights Regarding Core Stalling and Dynamical Buoyancy, Astrophys. J. **912**, 43 (2021), arXiv:2103.05004 [astro-ph.GA].

[25] U. Banik and F. C. van den Bosch, Dynamical Friction, Buoyancy, and Core-stalling. I. A Nonperturbative Orbit-based Analysis, Astrophys. J. **926**, 215 (2022), arXiv:2112.06944 [astro-ph.GA].

[26] J. I. Read, T. Goerdt, B. Moore, A. P. Pontzen, J. Stadel, and G. Lake, Dynamical friction in constant density cores: a failure of the Chandrasekhar formula, MNRAS **373**, 1451 (2006), arXiv:astro-ph/0606636 [astro-ph].

[27] T. Goerdt, B. Moore, J. I. Read, and J. Stadel, Core Creation in Galaxies and Halos Via Sinking Massive Objects, Astrophys. J. **725**, 1707 (2010), arXiv:0806.1951 [astro-ph].

[28] S. Inoue, Corrective effect of many-body interactions in dynamical friction, MNRAS **416**, 1181 (2011), arXiv:0912.2409 [astro-ph.CO].

[29] D. R. Cole, W. Dehnen, J. I. Read, and M. I. Wilkinson, The mass distribution of the Fornax dSph: constraints from its globular cluster distribution, MNRAS **426**, 601 (2012), arXiv:1205.6327 [astro-ph.CO].

[30] N. Dalal, Y. Lithwick, and M. Kuhlen, The Origin of Dark Matter Halo Profiles, arXiv e-prints , arXiv:1010.2539 (2010), arXiv:1010.2539 [astro-ph.CO].

[31] S. Tremaine and M. D. Weinberg, Dynamical friction in spherical systems., MNRAS **209**, 729 (1984).

[32] M. D. Weinberg, Self-gravitating response of a spherical galaxy to sinking satellites, MNRAS **239**, 549 (1989).

[33] K. Kaur and S. Sridhar, Stalling of Globular Cluster Orbits in Dwarf Galaxies, Astrophys. J. **868**, 134 (2018), arXiv:1810.00369 [astro-ph.GA].

[34] K. Kaur and N. C. Stone, Density wakes driving dynamical friction in cored potentials, MNRAS **515**, 407 (2022), arXiv:2112.10801 [astro-ph.GA].

[35] P. H. Diamond, S.-I. Itoh, and K. Itoh, *Modern Plasma Physics* (Cambridge University Press, 2010).

[36] A. N. Kaufman, Quasilinear Diffusion of an Axisymmetric Toroidal Plasma, Physics of Fluids **15**, 1063 (1972).

[37] J. Binney and S. Tremaine, *Galactic Dynamics: Second Edition, by James Binney and Scott Tremaine. ISBN 978-0-691-13026-2 (HB). Published by Princeton University Press, Princeton, NJ USA, 2008.* (Princeton University Press, 2008).

[38] W. Dehnen, A Family of Potential-Density Pairs for Spherical Galaxies and Bulges, MNRAS **265**, 250 (1993).

[39] A. J. Kalnajs, Dynamics of flat galaxies. IV. The integral equation for normal modes in matrix form., Astrophys. J. **212**, 637 (1977).